STUDIES ON CAMPYLOBACTER SPUTORUM SUBSPECIES MUCOSALIS INFECTION IN PIGS.

VOLUME II

ELINOR McCARTNEY
B.V.M.&S., M.R.C.V.S.

AUGUST, 1982

Degree of Doctor of Philosophy, Department of Veterinary Pathology, University of Edinburgh.

"A picture may instantly present what a book could set forth only in a hundred pages."

- Ivan Sergeyevich Turgenev

Figure 1.1. The typical appearance of a weaner pig with PIA. The animal is poorly-fleshed and has a rough coat.

Figure 1.2. Porcine intestinal adenomatosis - gross appearance of the gut at necropsy. The terminal small intestine and caecum are opened to show a thickened, corrugated mucosa.

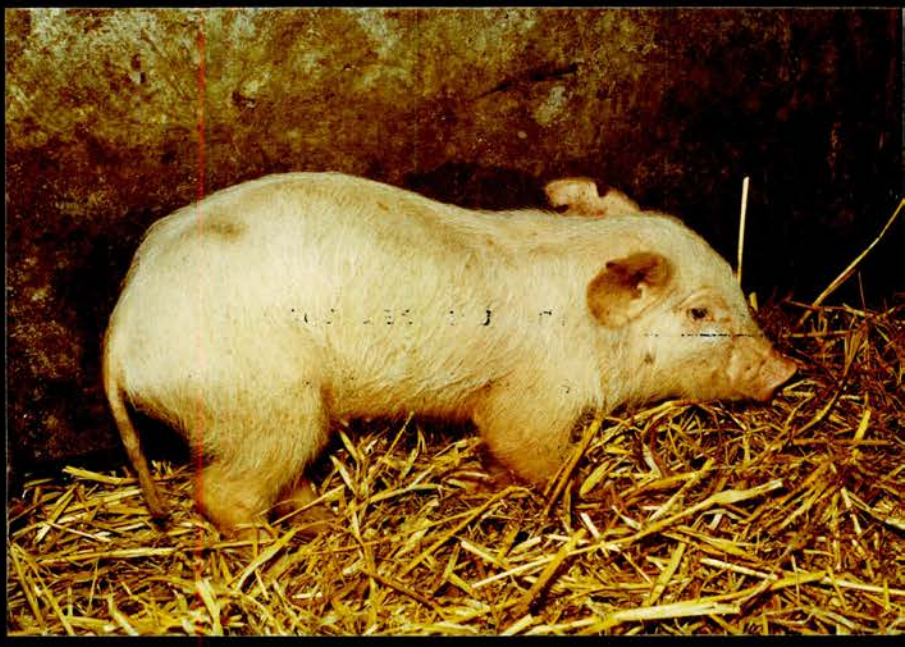

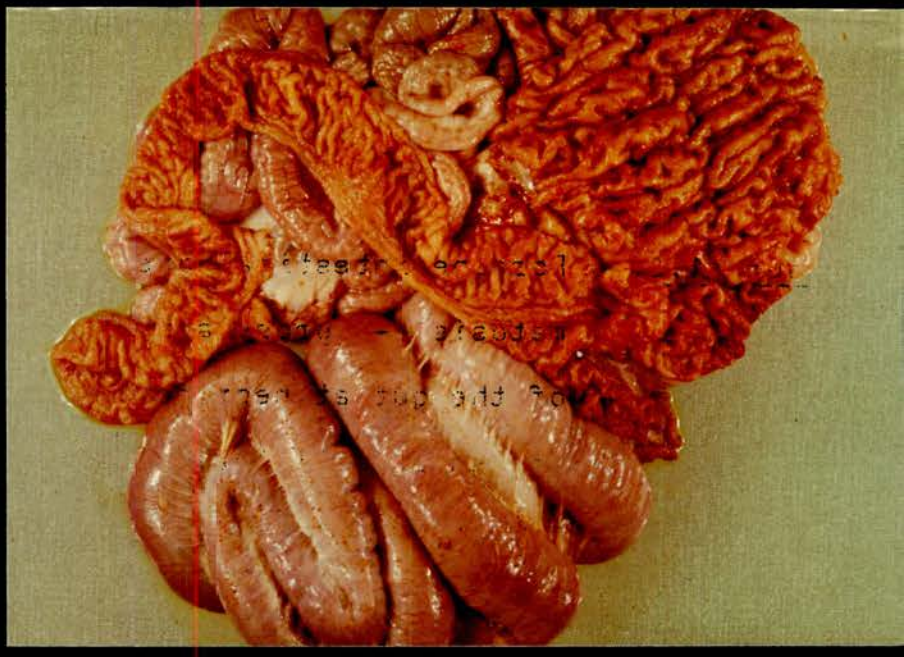

Figure 1.3. Close-up of an adenomatous ileum. Note the oedematous mesentery, the patches of subserosal oedema and the thickened reticulate mucosa.

Figure 1.4. Terminal small intestine showing adenomatous areas appearing as polypoid growths contrasting markedly with normal mucosa.

Figure 1.5. Normal terminal ileum in a weaned pig. Conical villi overly simple tubular crypt glands. Note the abundant goblet cells and the lymphoid follicles beneath the muscularis mucosae.
H. & E. x 100.

Figure 1.6. Adenomatous mucosa in a weaned pig. Note the absence of villi and goblet cells. The mucosa consists of enlarged, mis-shapen crypt glands.
H. & E. x 100.

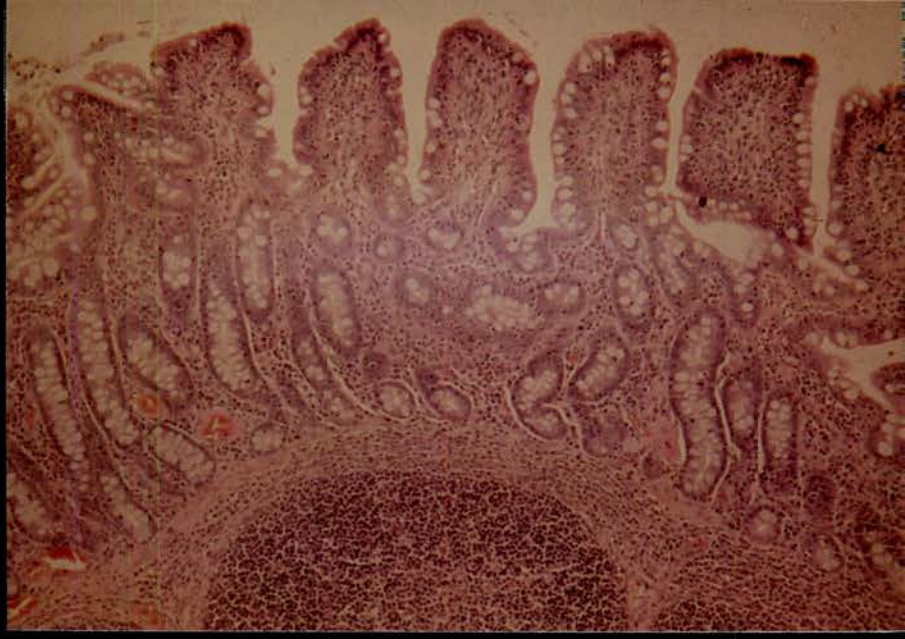

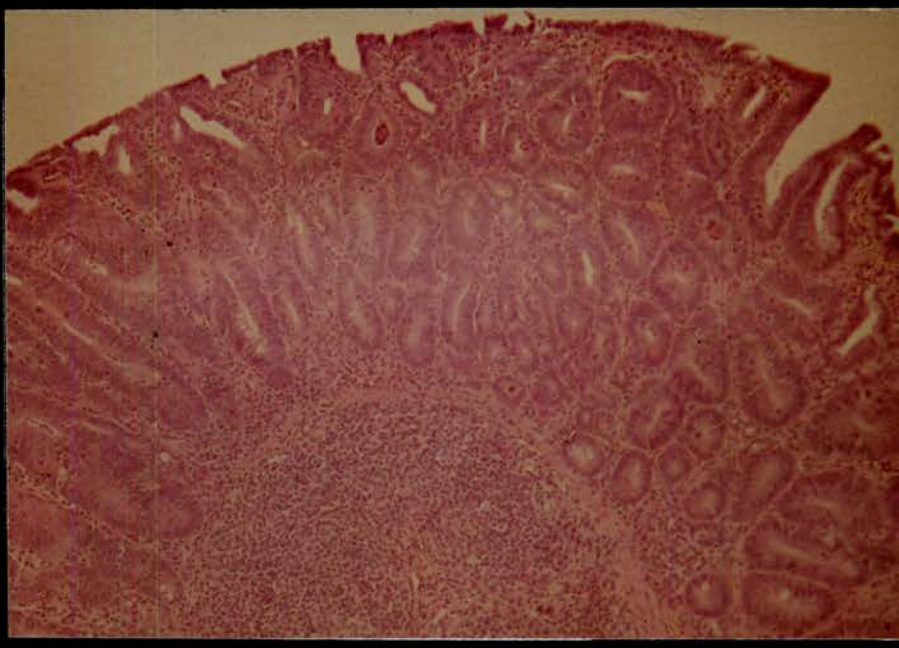

Figure 1.7. Large bowel from a weaned pig with PIA. Note the abrupt change from adenomatous glands to more normal glands containing goblet cells. H. & E. x 70.

Figure 1.8. High power of adenomatous glands showing tortuous, branching nature and "crowded" appearance of the proliferating crypt cells. Note the relative lack of inflammatory cells in the lamina propria. H. & E. x 200.

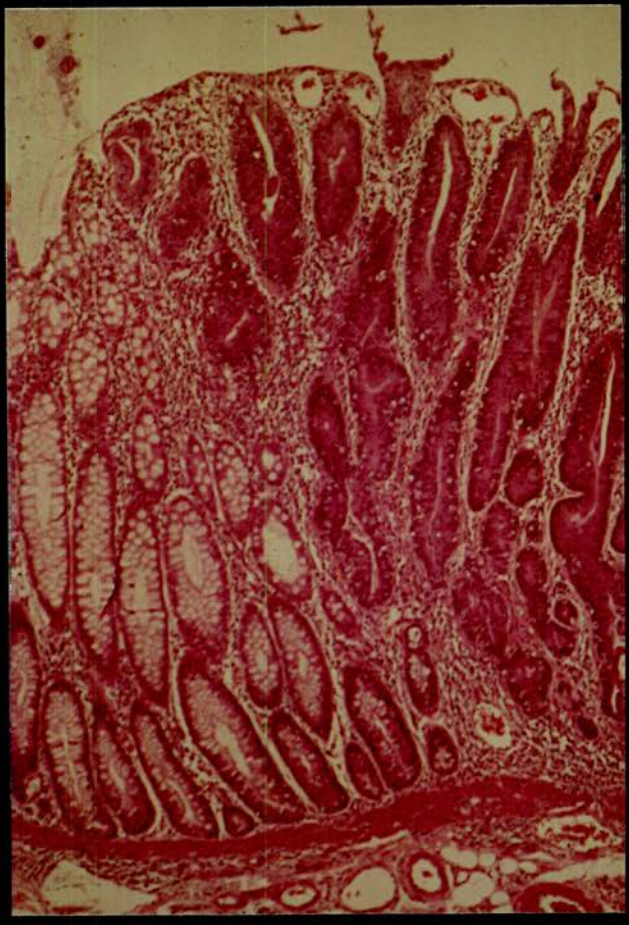

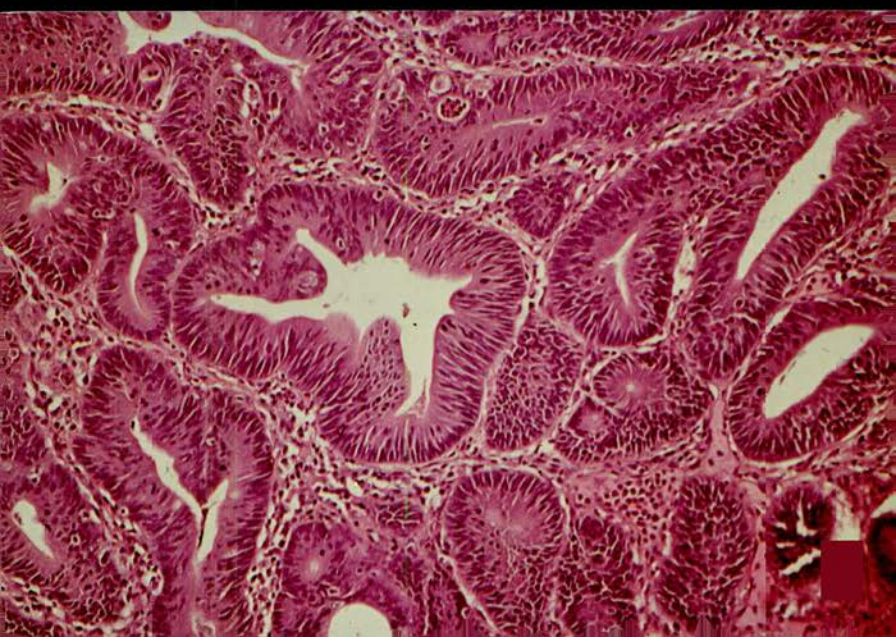

Figure 1.9. Scanning electron micrograph of adenomatous mucosa in the small intestine. Note the absence of villi and the elongate nature of exposed crypt glands (extreme left). The surface is free of the inflammatory debris.
Bar = 400 μm
Final magnification = 30.


400UM 30KV 01/ 001 S

Figure 1.10. Scanning electron micrograph of normal small intestine. The villi are well-formed and exhibit occasional goblet cells. Compare with Figure 1.11.
Bar = 40μm.
Final magnification = 360.

Figure 1.11. Scanning electron micrograph of adenomatous mucosa taken at same magnification as Figure 1.10. Goblet cells are absent. The surface is largely free of inflammatory debris.
Bar = 40μm.
Final magnification = 360.

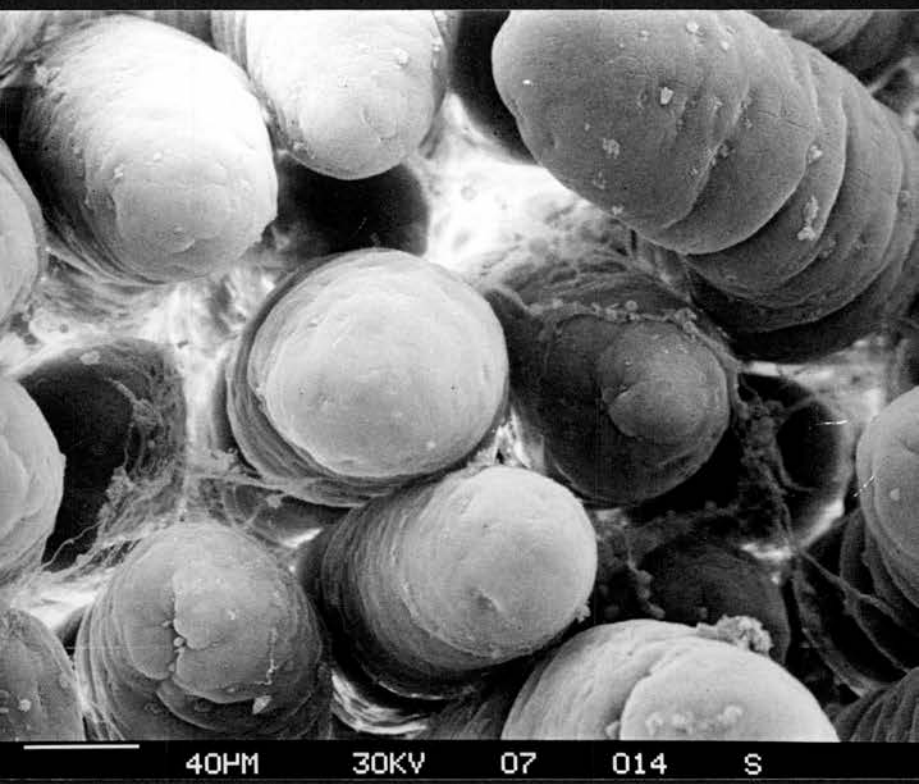
40PM 30KV 07 014 S

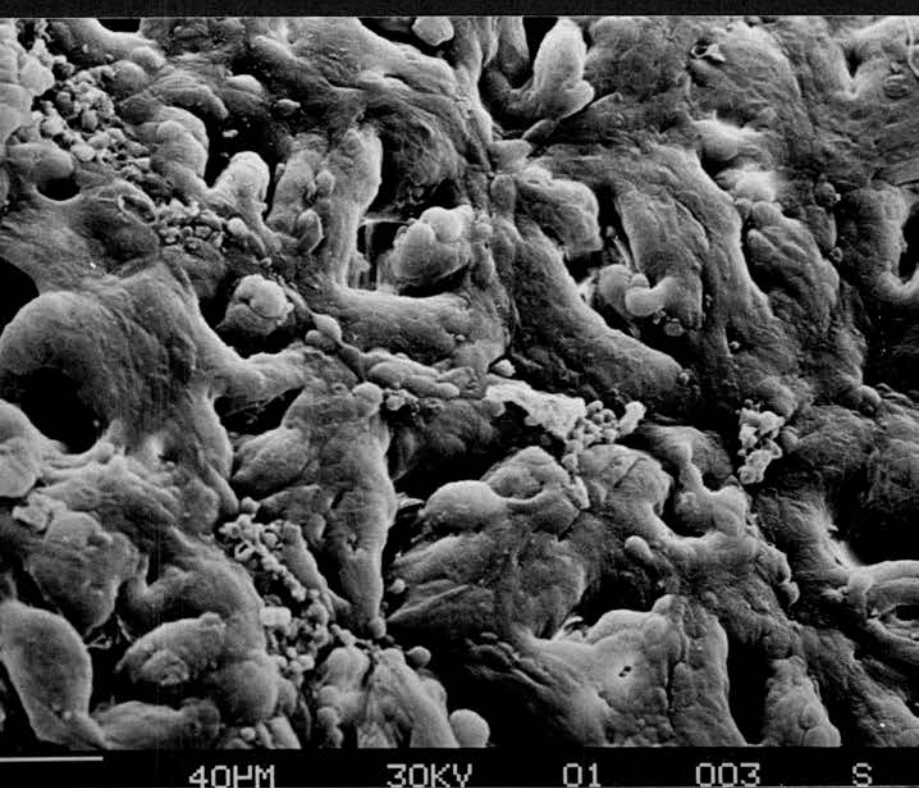
40PM 30KV 01 003 S

Figure 1.12. High power scanning electron micrograph of the surface of adenomatous cells. Note the sparse, poorly developed microvilli, a feature of immature enterocytes. Compare with Figure 1.13. Bar = 1μm. Final magnification = 13,000.

Figure 1.13. High power scanning electron micrograph of normal mature enterocytes. Note abundant, well-developed microvilli. Taken at same power as Figure 1.12. Bar = 1μm. Final magnification = 13,000.

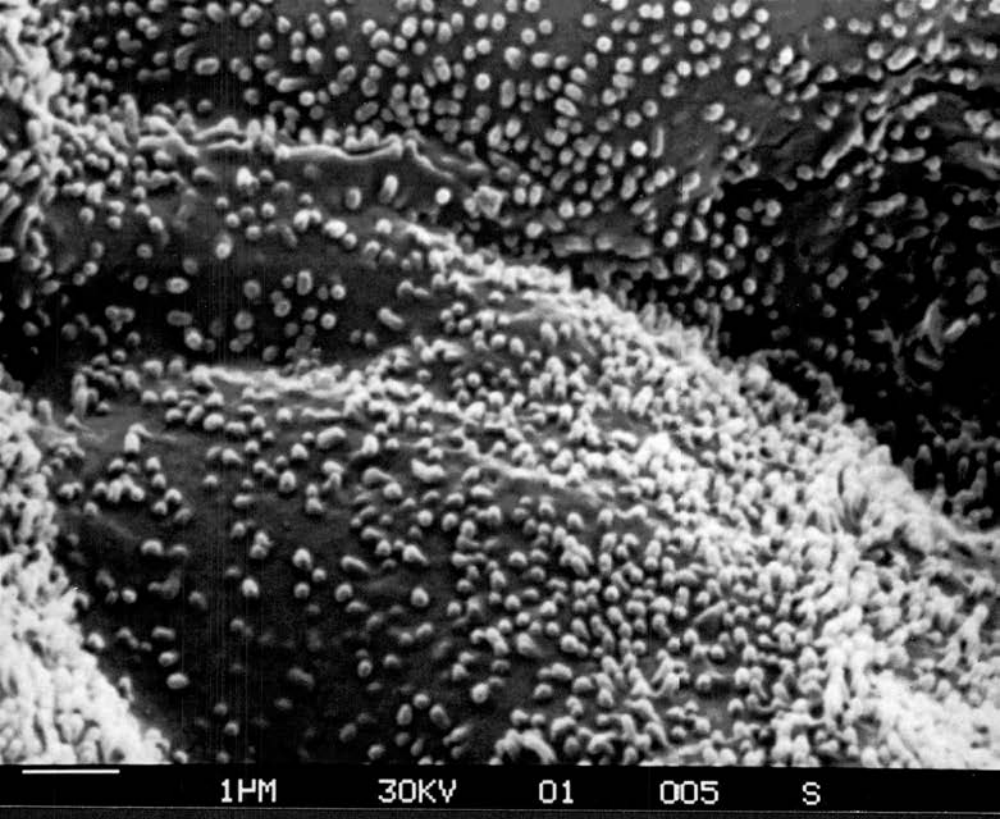
1μM 30KV 01 005 S

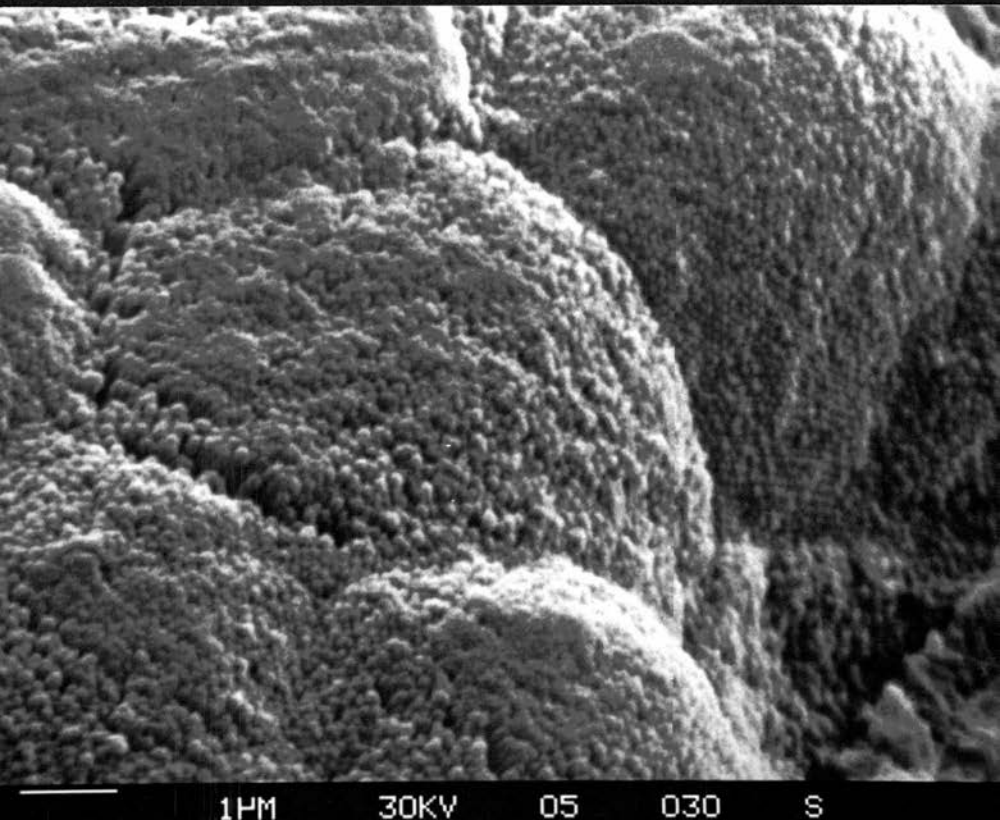
1μM 30KV 05 030 S

Figure 1.14. Levaditi stain of adenomatous gland. Numerous argyrophilic bacteria concentrated in the apical cytoplasm of host cells.
Final magnification = 1,020.

Figure 1.15. Young's stain showing argyrophilic forms resembling campylobacters in the apical cytoplasm of adenomatous cells.
Final magnification = 625.

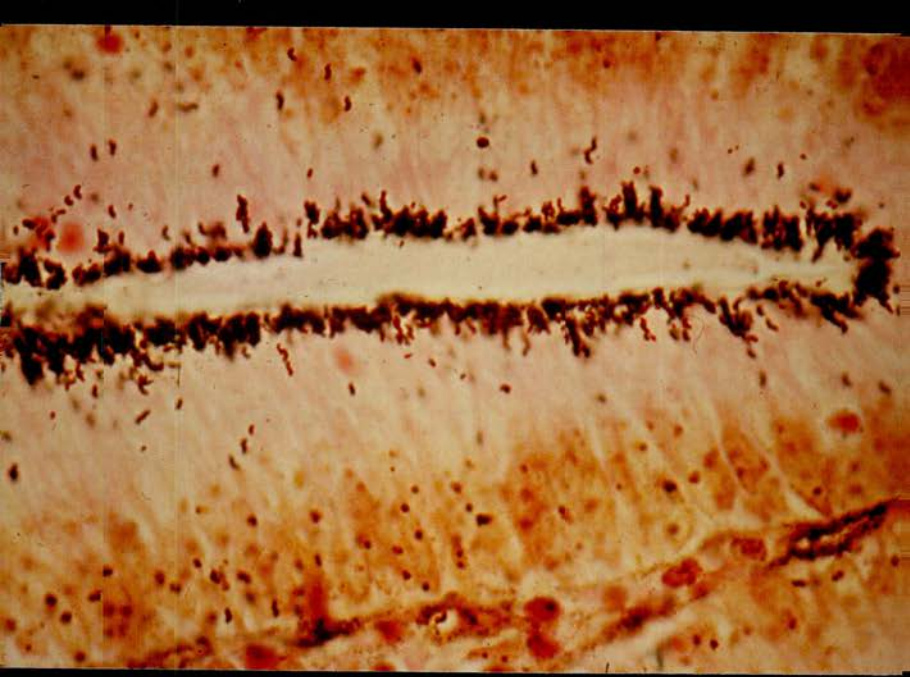

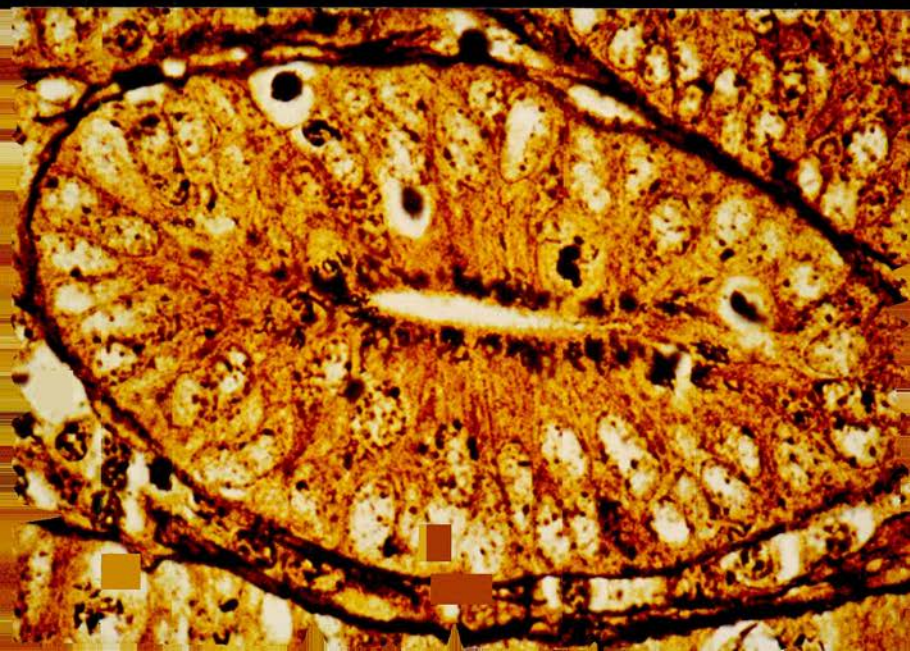

Figure 1.16. Kerr's stain of adenomatous cells. Note improved definition of the densely-stained irregularly curved bacterial forms. Thin section.
Final magnification = 1,400.

Figure 1.17. Uncomplicated and early adenomatous change in a crypt gland. Affected cells have campylobacter-like bacteria in the cell cytoplasm. Goblet cells still present.
Final magnification = 6,500.

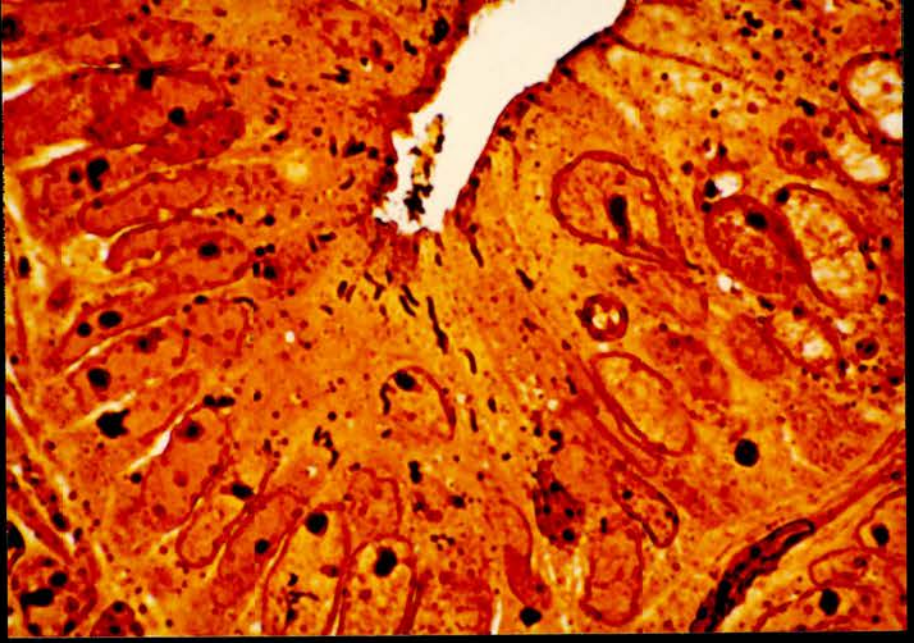

Figure 1.18. Intracellular bacteria in an adenomatous cell. The bacteria lie free in the cytoplasm.
Final magnification = 24,000.

Figure 1.19. High power transmission electron micrograph showing the absence of host-cell membranes surrounding the bacteria which have typical campylobacter morphology.
Final magnification = 70,000.

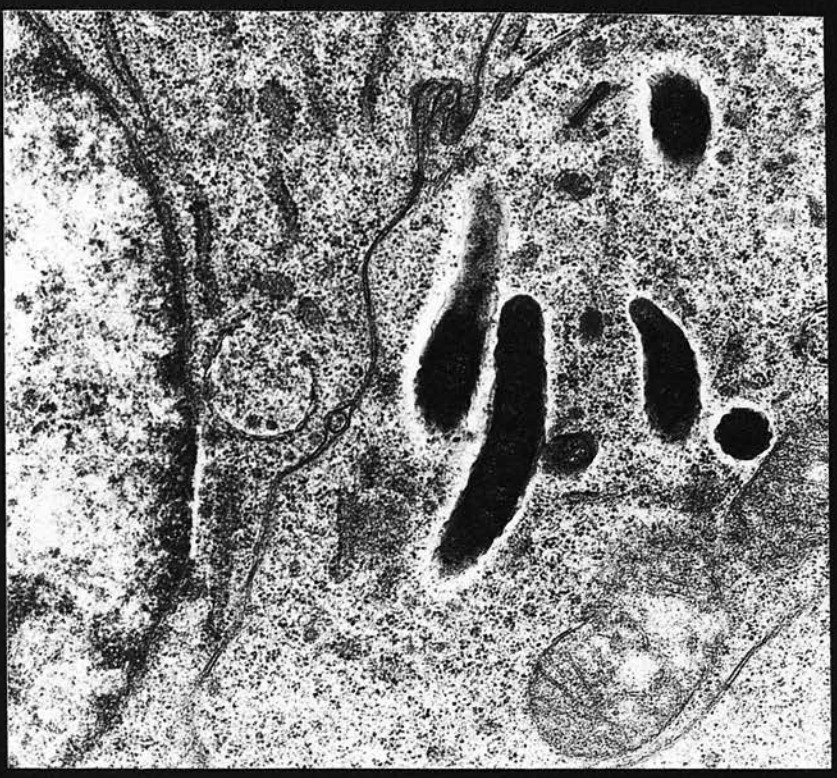

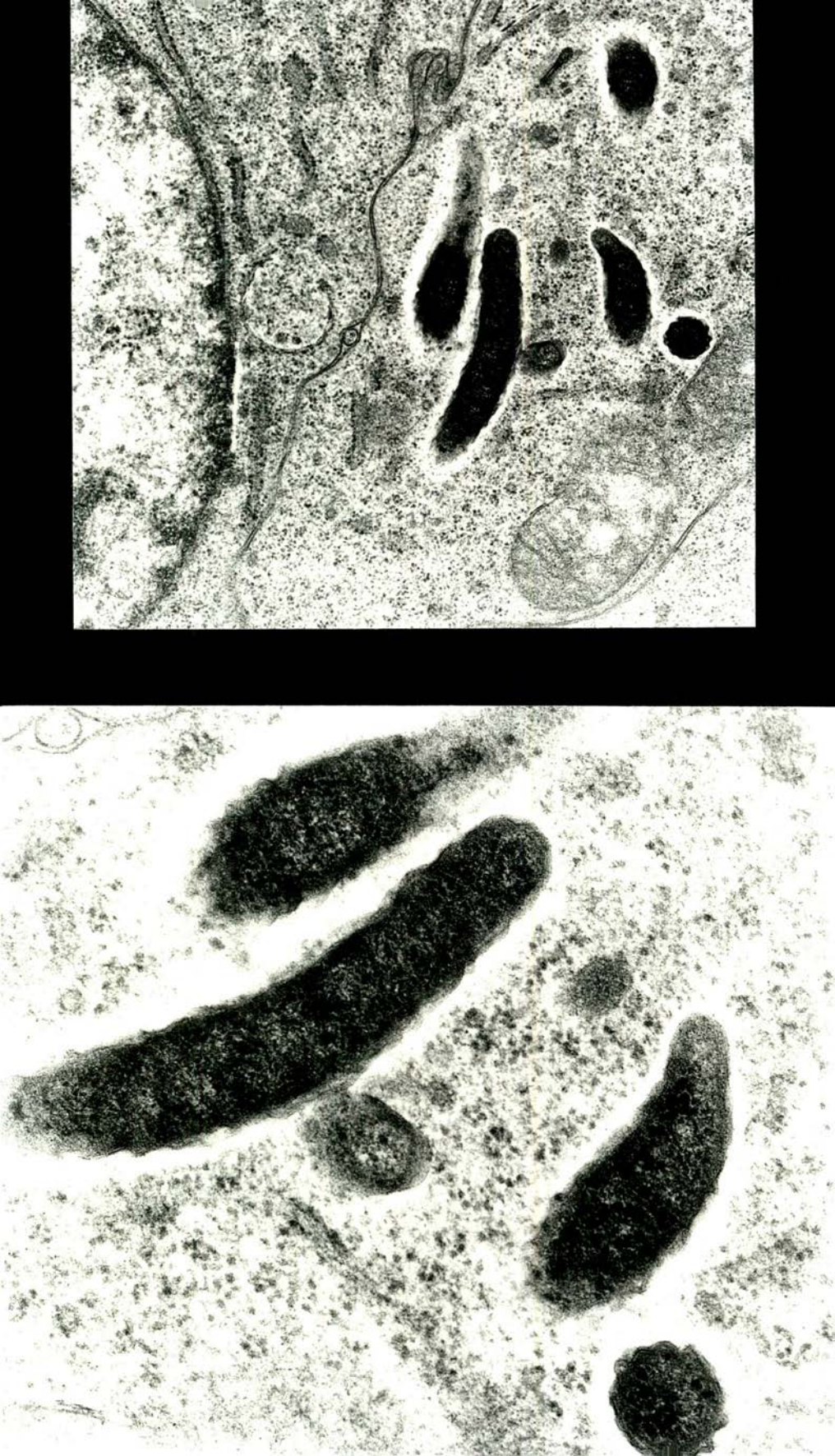

Figure 1.20. Smear of *mucosalis* from a 48 hour culture. Gram stain. Final magnification = 1,200.

Figure 1.21. Adenomatous glands stained by immunofluorescence technique for serotype A *mucosalis*. Note bright, sometimes particulate nature of the fluorescence concentrated in the apical cytoplasm of affected cells.
Final magnification = 300.

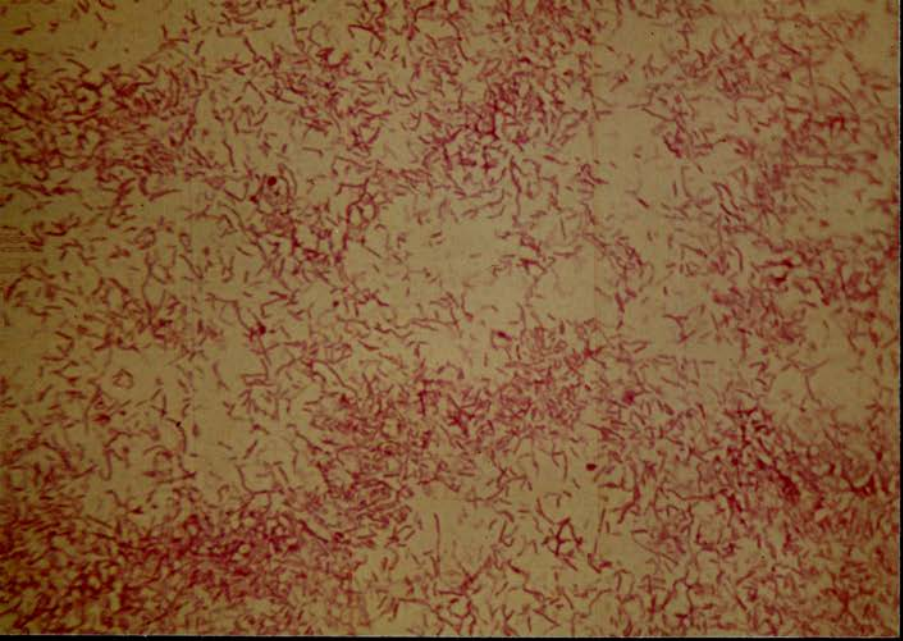

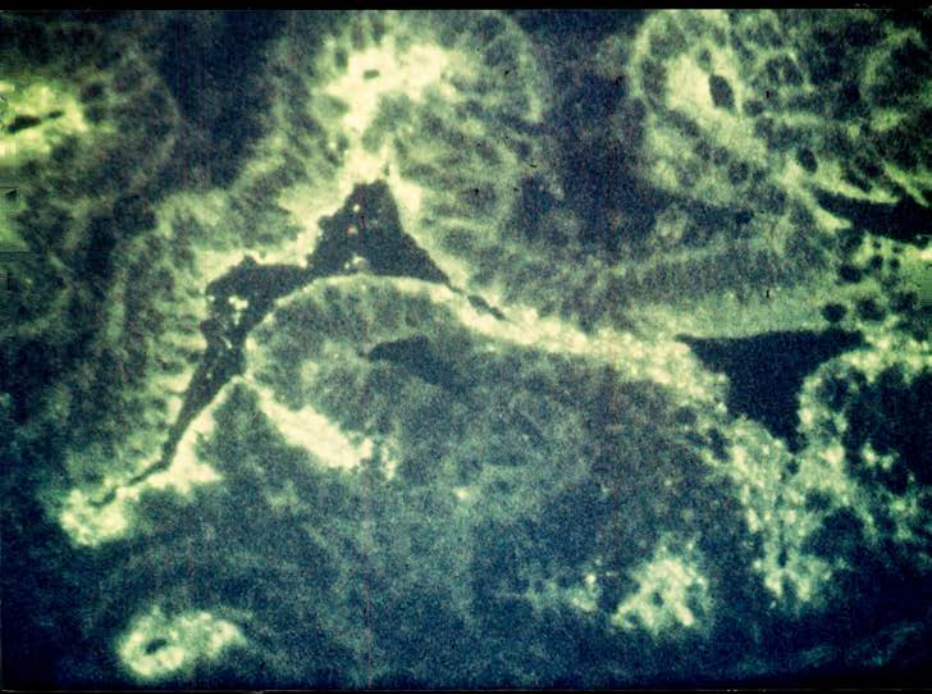

Figure 2.1. Piglet under terminal anaesthesia. Samples have been taken from the small bowel.

Figure 3.2. Kerr's stain. Piglet A46. MSl. Villar enterocytes showing numerous pleomorphic argyrophilic bodies in the apical cytoplasm. Final magnification = 870.

Figure 3.3. Piglet A46. MS1. Villar enterocytes with electron-dense pleomorphic bodies in the apical cytoplasm. Final magnification = 5,500.

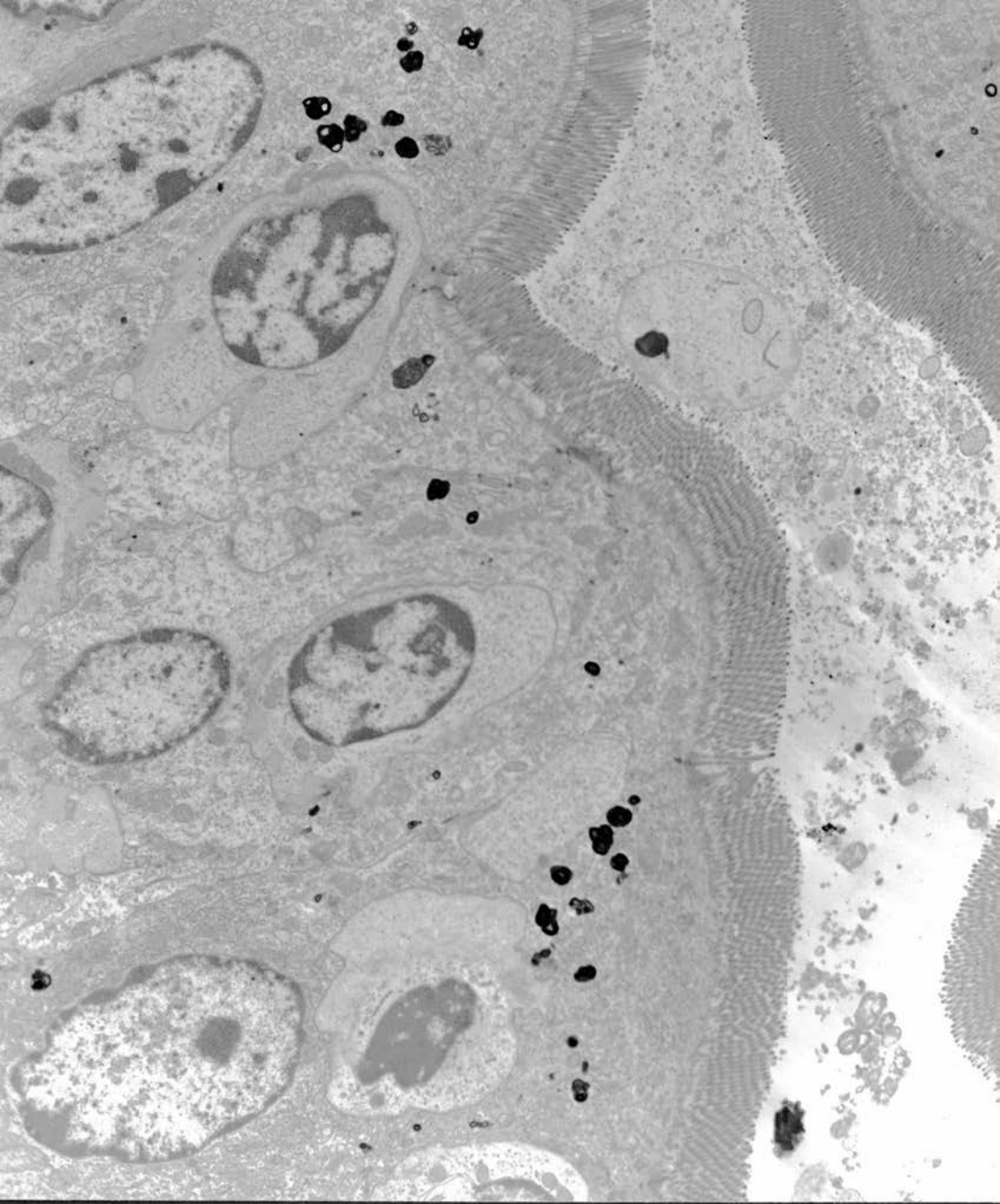

Figure 3.4. Piglet A38, TS1. High power of pleomorphic electron-dense bodies in apical cytoplasm of a villar enterocyte.
Final magnification = 92,000.

Figure 3.5. Piglet A38. TS1. High power of intracellular body showing lamellar structure typical of myelinosome.
Final magnification = 92,000.

Figure 3.6. Piglet A46. MS1. Cytoplasm of villar enterocyte showing electron-dense body of similar morphology to a campylobacter but lacking characteristic cell wall structure. Final magnification = 92,000.

Figure 3.7. Piglet A46. MS1. High power of electron-dense body in villar enterocyte. Although bearing a superficial resemblance to a campylobacter, the body lacks the characteristic cell wall structure.
Final magnification = 200,000.

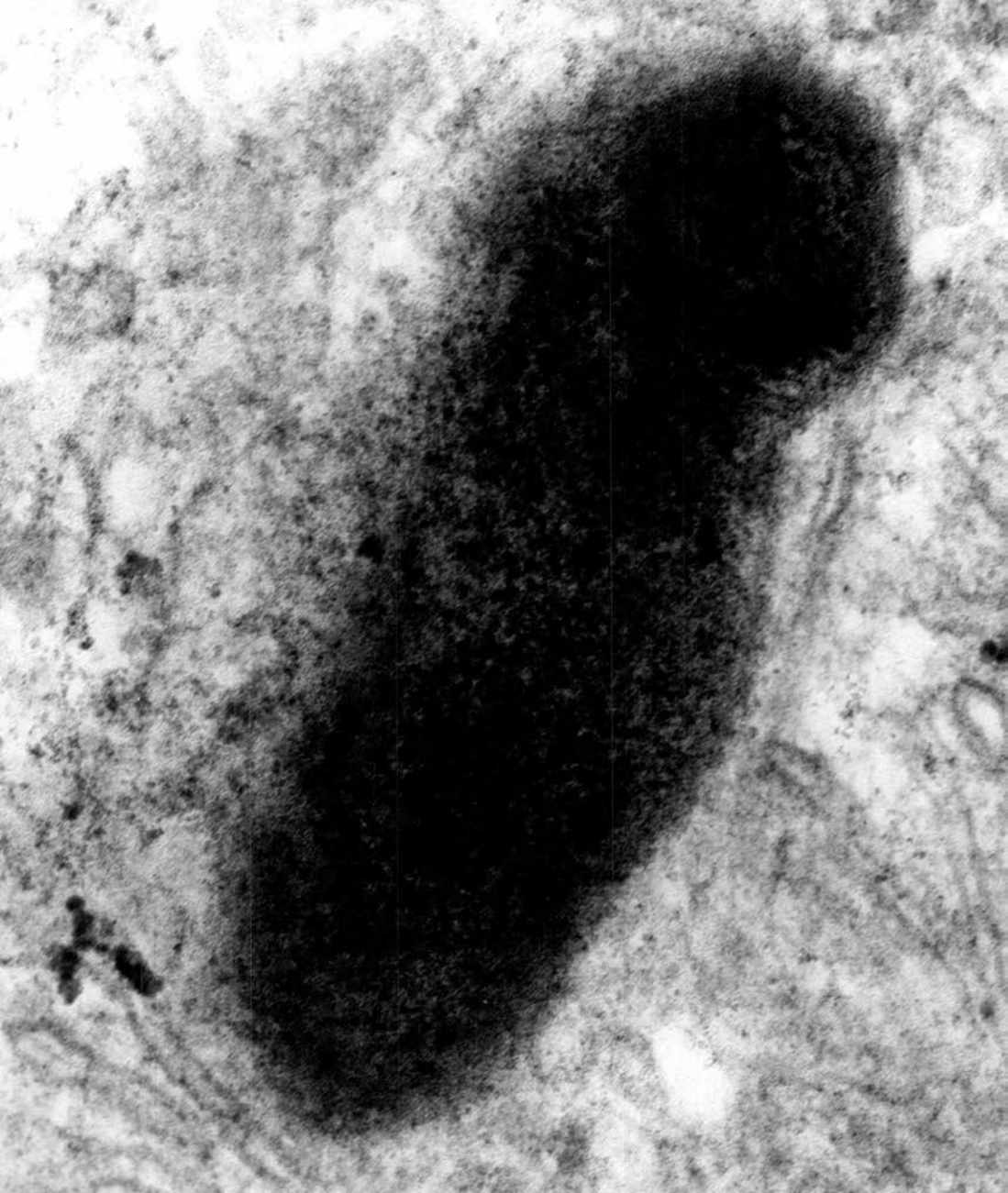

Figure 4.1. MSl of a 10 day old colostrum-fed piglet showing heavily vacuolated villar enterocytes. H. & E. x 60.

Figure 4.2. MSl of colostrum-deprived piglet C2, 10 days old. Note the absence of vacuoles in the villar enterocytes. H. & E. x 60.

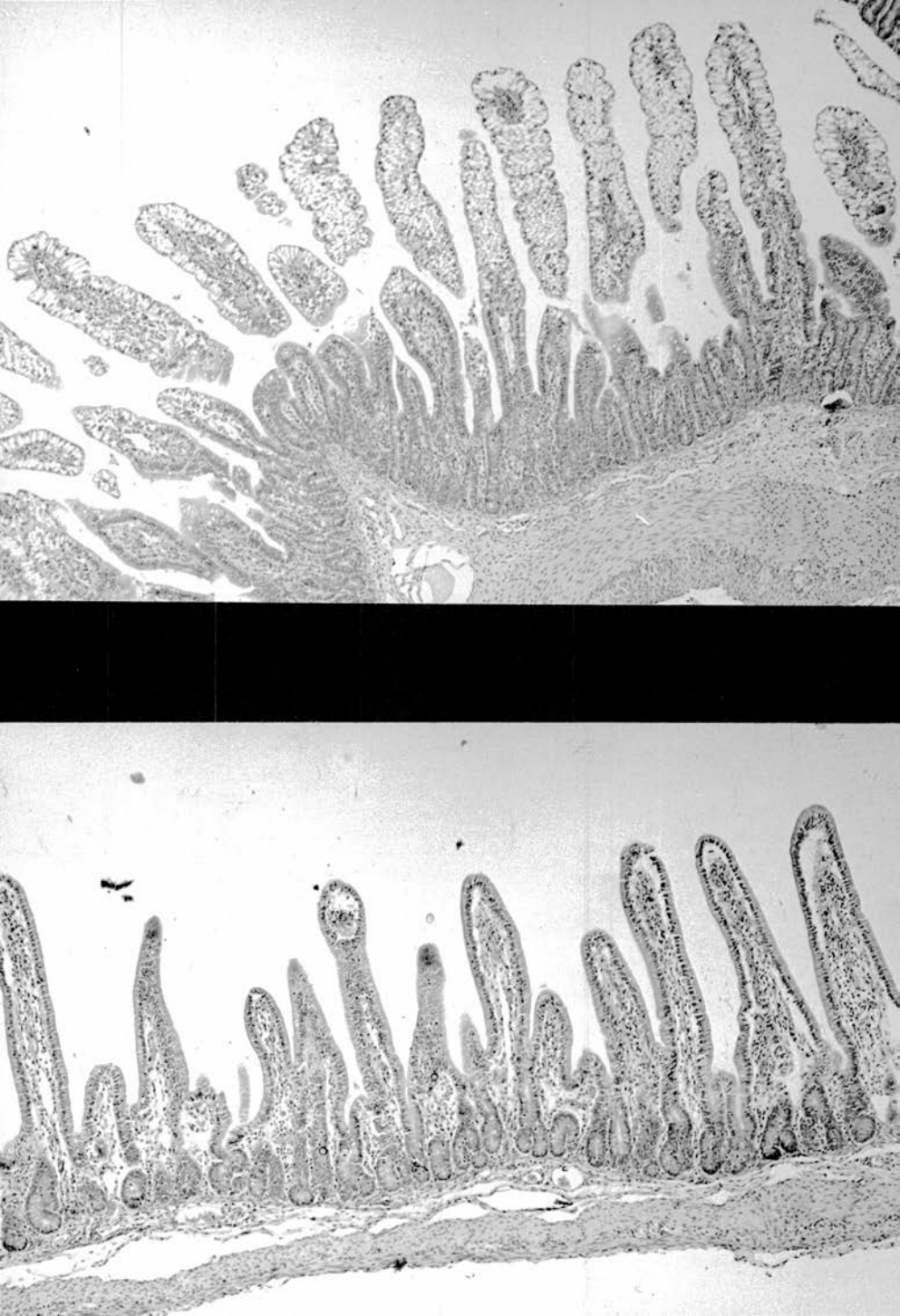

Figure 4.3. MSl of exposed piglet F5, 11 days old. There is blunting, fusion and loss of villi, increased cellularity of the lamina propria and inflammatory cells and debris in the gut lumen. H. & E. x 60.

Figure 4.4. LB of exposed piglet F5, 11 days old. There is extrusion of surface cells, depletion of goblet cells and an increased number of inflammatory cells and the pyknotic debris in the lamina propria and crypts. H. & E. x 155.

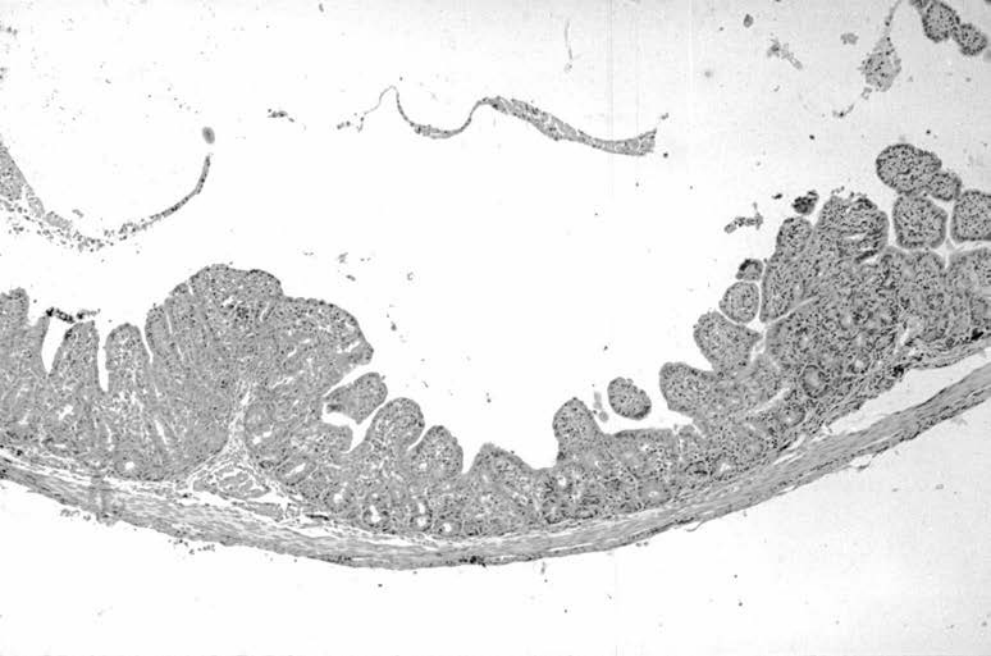

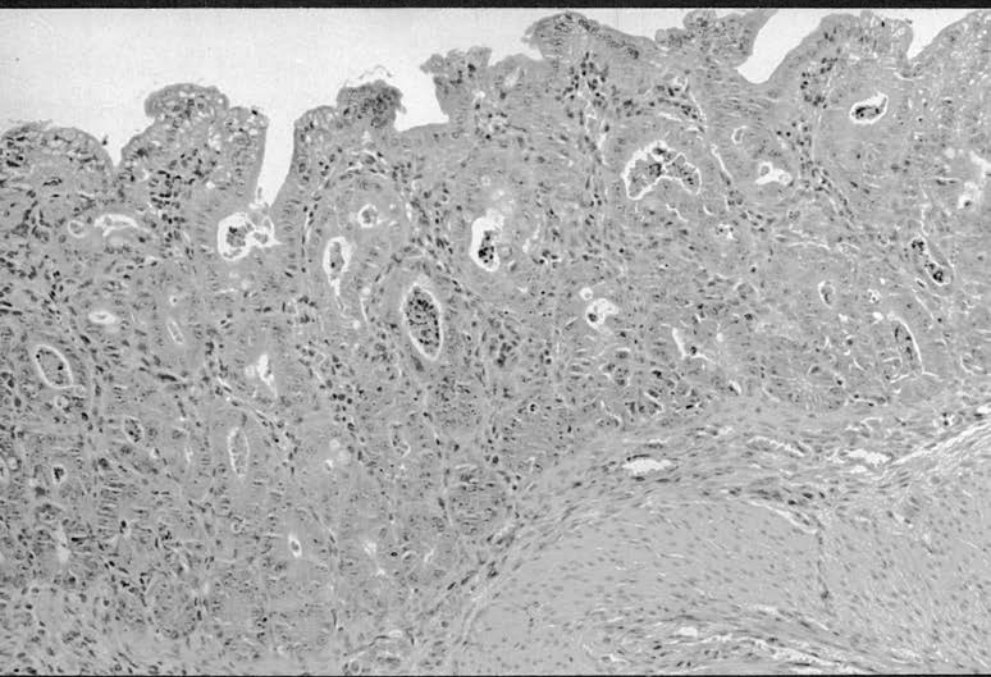

Figure 4.5. LB of exposed piglet F1. Note the presence of intracellular profiles resembling campylobacters. Kerr's x 1,480.

Figure 4.6. LB of exposed piglet F1. Campylobacter-like bacteria are present in the crypt lumen. Kerr's x 1,515.

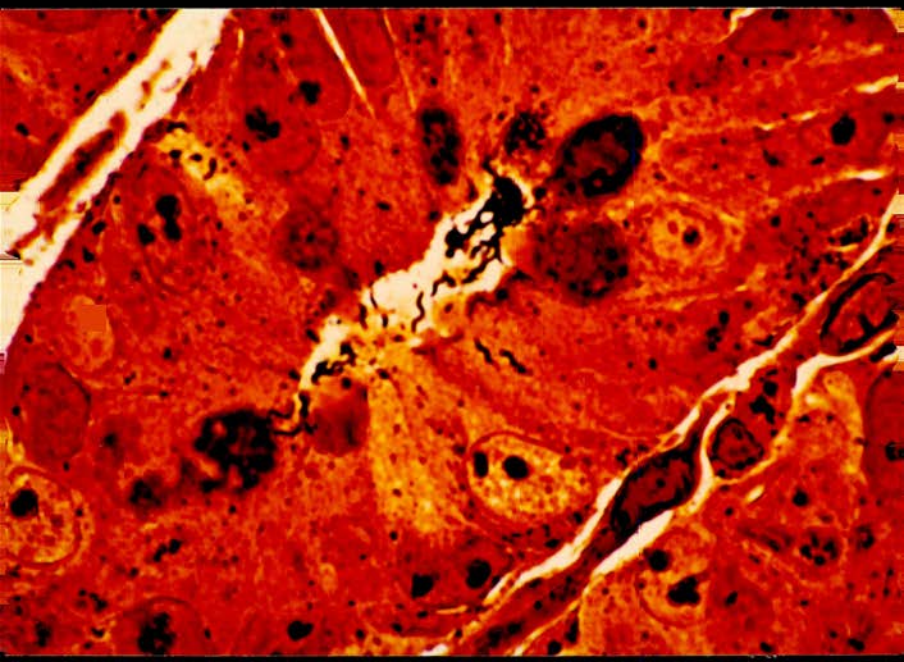

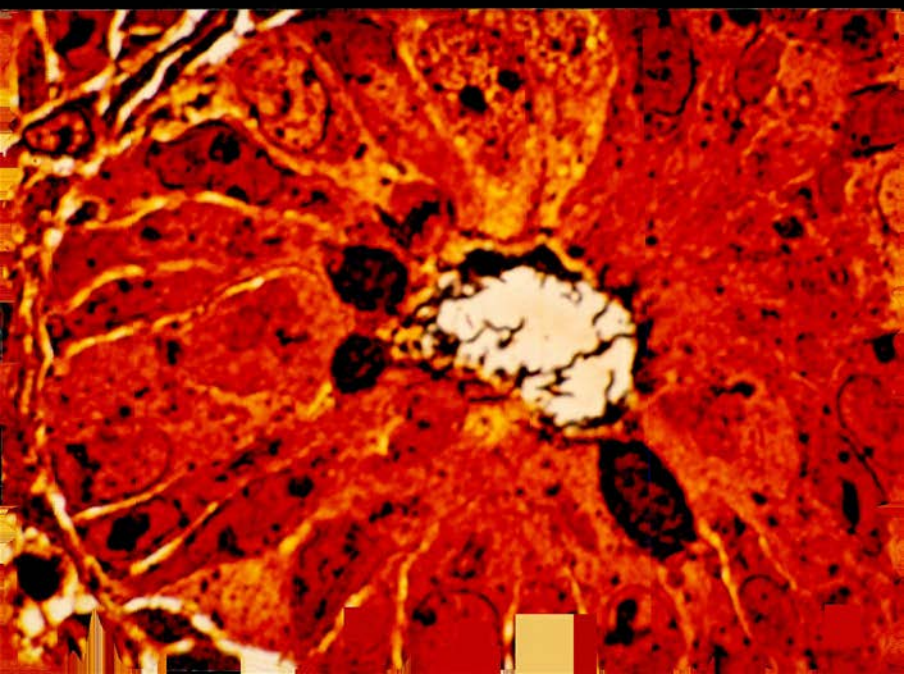

Figure 4.7. TSl of exposed piglet F5, stained for Serotype A mucosalis. There is bright diffuse fluorescence in the lumina of basal crypts. Final magnification = 770.

Figure 4.8. LB of control piglet C3. Campylobacter-like organisms in the lumina of a crypt but not adhering to the surface of host cells. Final magnification = 18,900.

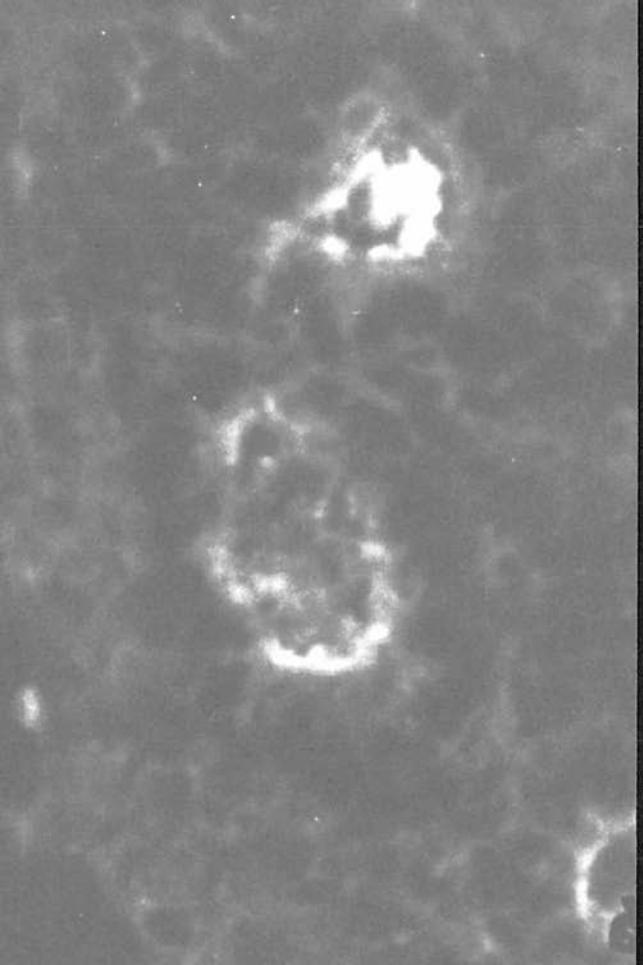

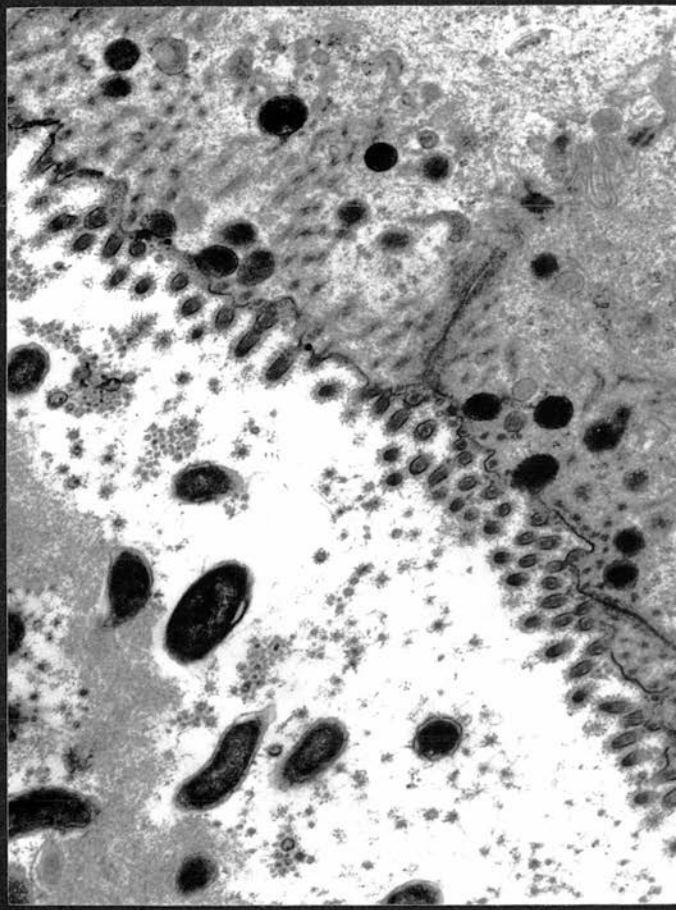

Figure 4.9. LB of exposed piglet F1 showing close association between bacteria resembling campylobacters and host epithelial cells.
Final magnification = 15,000.

Figure 4.10. LB of exposed piglet F1.
Campylobacter-like organism close to host microvilli.
Final magnification = 19,500.

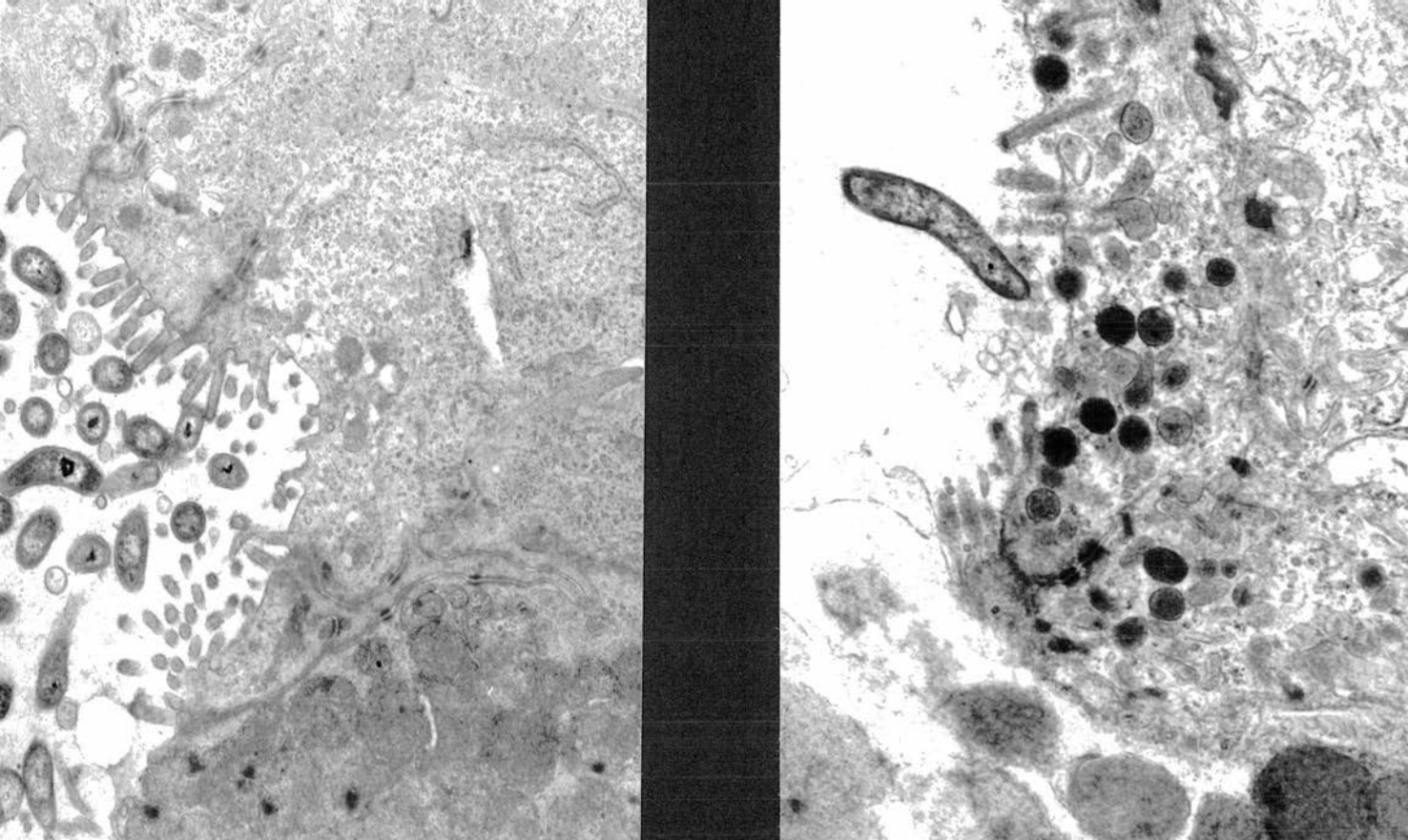

Figure 4.11. Higher power of Figure 4.10 showing presence of a single polar flagellum, a typical morphological feature of campylobacters. Note proximity to host-cell membrane.
Final magnification = 56,500.

Figure 4.12. LB of exposed piglet F1. A campylobacter-like organism is present deep in the cytoplasm of a crypt cell (lower left).
Final magnification = 7,000.

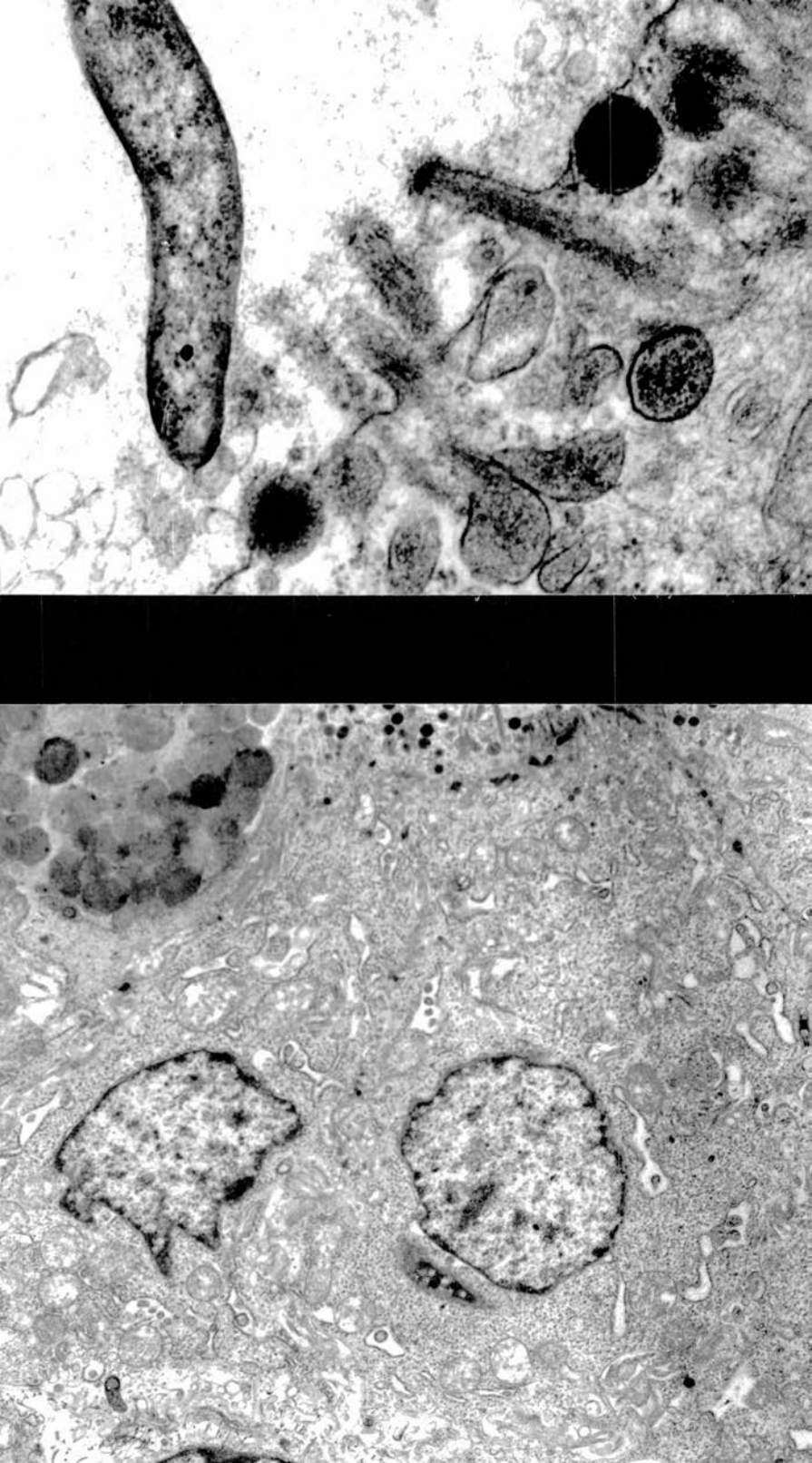

Figure 4.13. Higher power of Figure 4.12. Note the absence of host-cell membranes around the bacterium. Final magnification = 16,000.

Figure 4.14. Very high power of Figure 4.13 showing characteristic campylobacter morphology. Final magnification = 125,000.

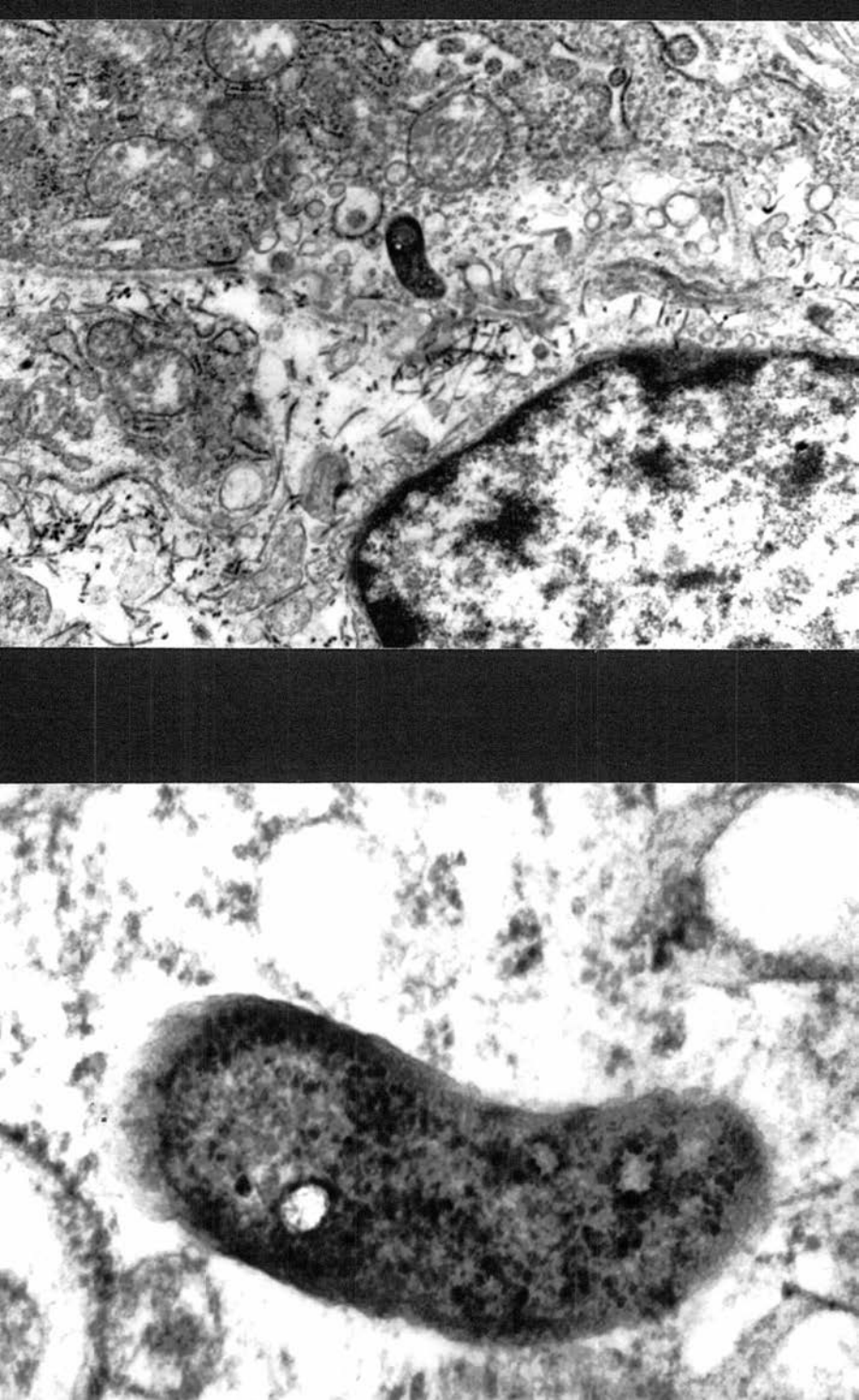

Figure 4.15. LB of exposed piglet F1. Lamina propria showing campylobacter-like organism free in the intercellular space in the vicinity of a blood vessel (upper left from blood vessel). Final magnification = 6,000.

Figure 4.16. LB of exposed piglet F1. Crypt lumen containing predominantly campylobacter-like bacteria. Note 2 campylobacter-like bacteria within a goblet cell (lower right). Final magnification = 12,000.

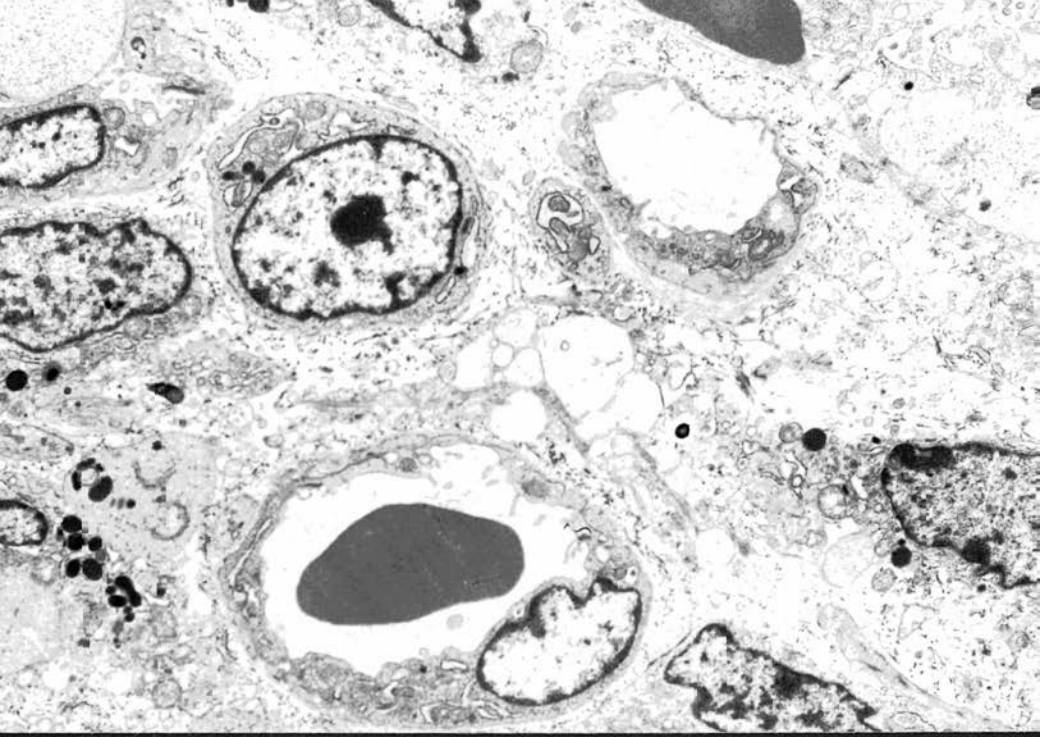

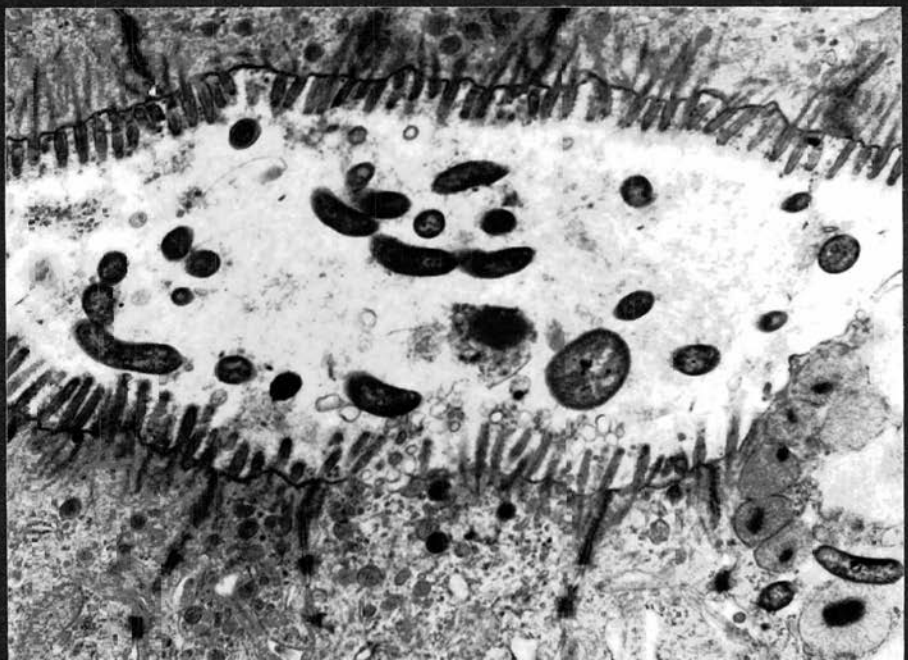

Figure 4.17. Same area as Figure 4.16 showing the 2 campylobacter-like bacteria lying between granules of mucus in a goblet cell.
Final magnification = 15,000.

Figure 4.18. MS1 of exposed piglet F5. Campylobacter-like bacteria in close association with microvilli of a host enterocyte.
Final magnification = 32,250.

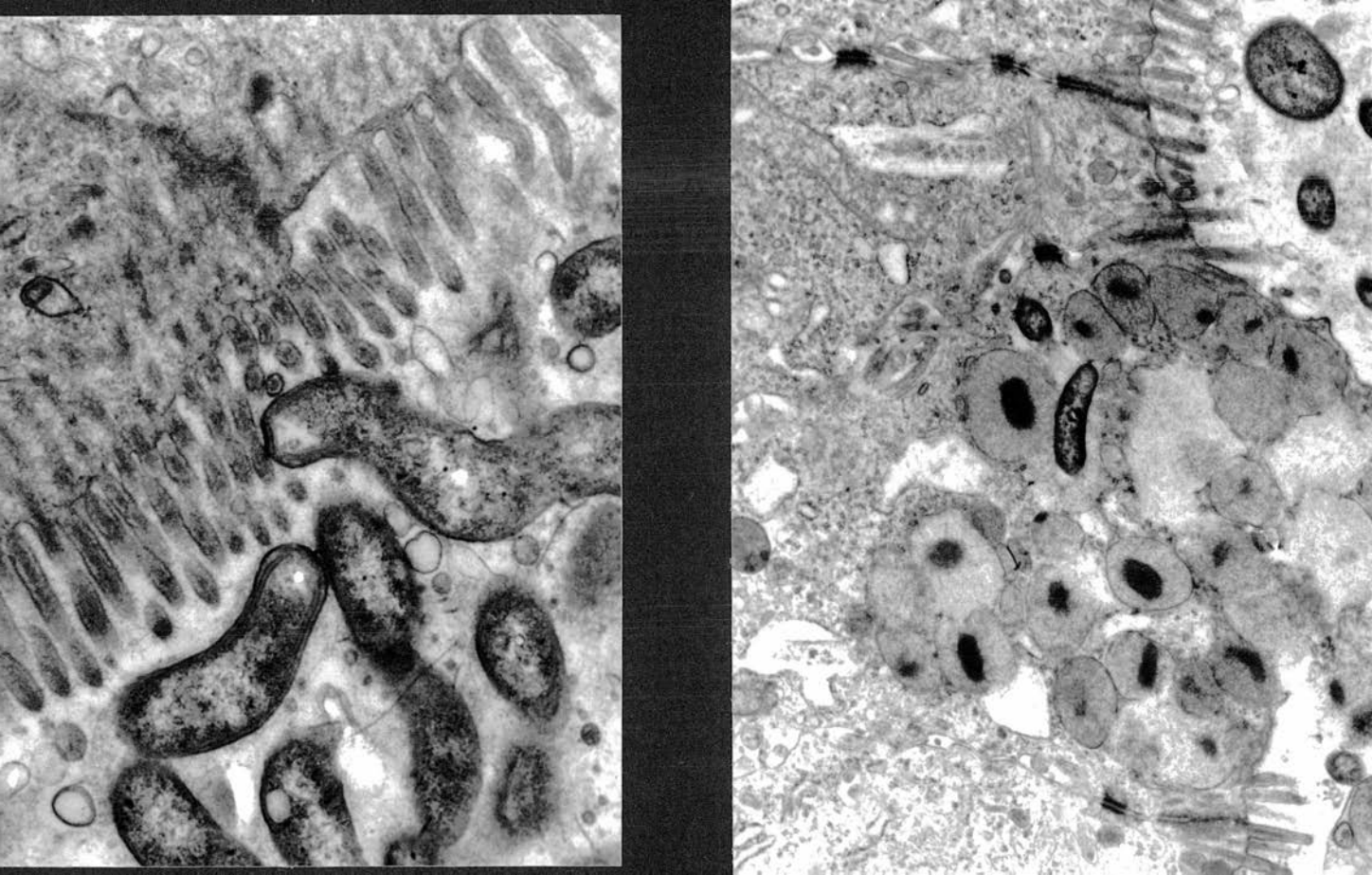

Figure 4.19. TS1 of exposed piglet F5 showing an evacuated goblet cell. Campylobacter-like organisms present (top left).
Final magnification = 18,750.

Figure 4.20. LB of exposed piglet F5 showing lamina propria at the base of a crypt. Bacteria of mixed morphology are free in the lamina propria.
Final magnification = 2,500.

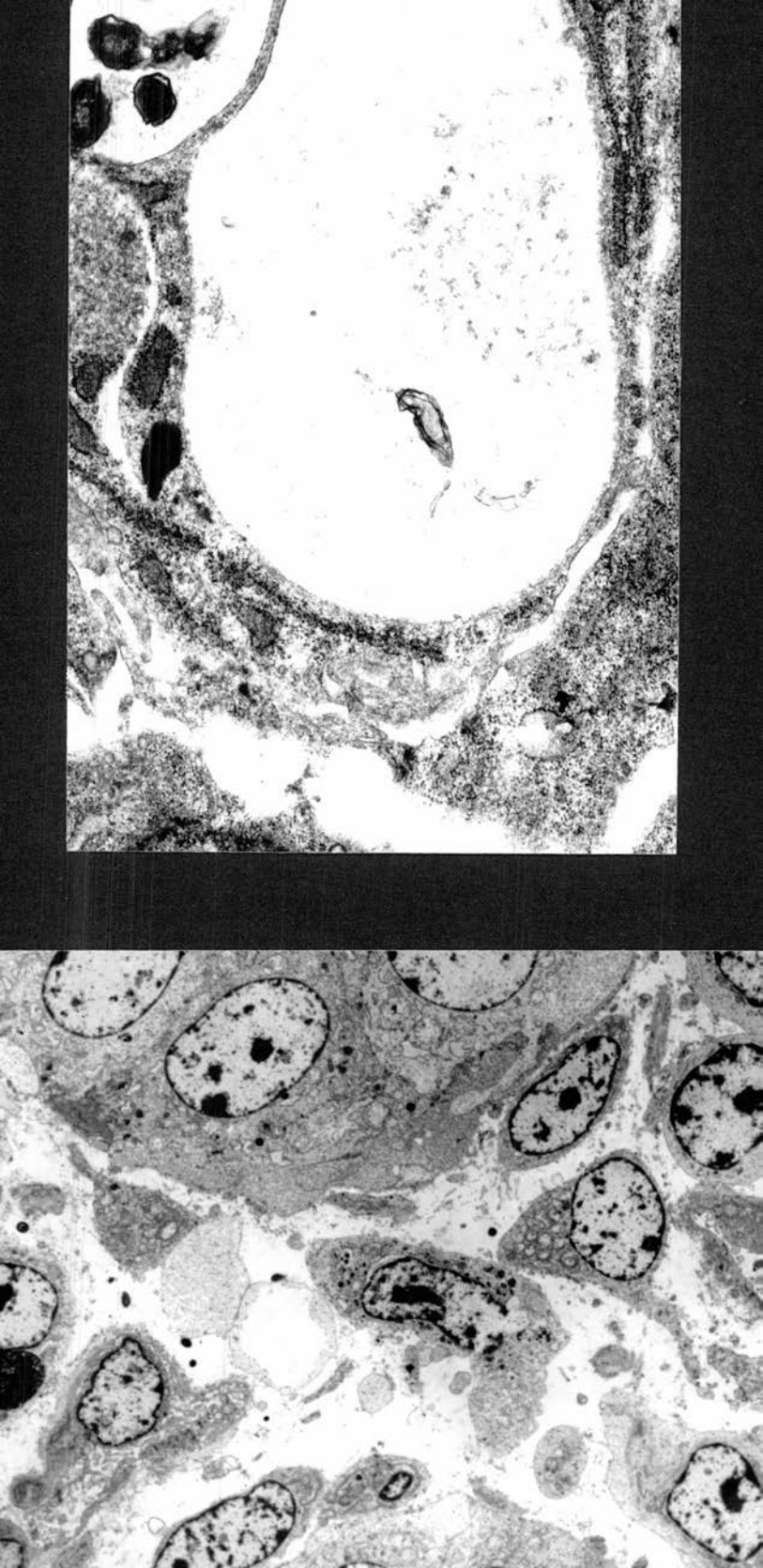

Figure 4.21. LB of exposed piglet F5 showing crypt lumen (top left) containing mixed bacterial flora and lamina propria (bottom right) containing occasional bacterial forms.
Final magnification = 5,000.

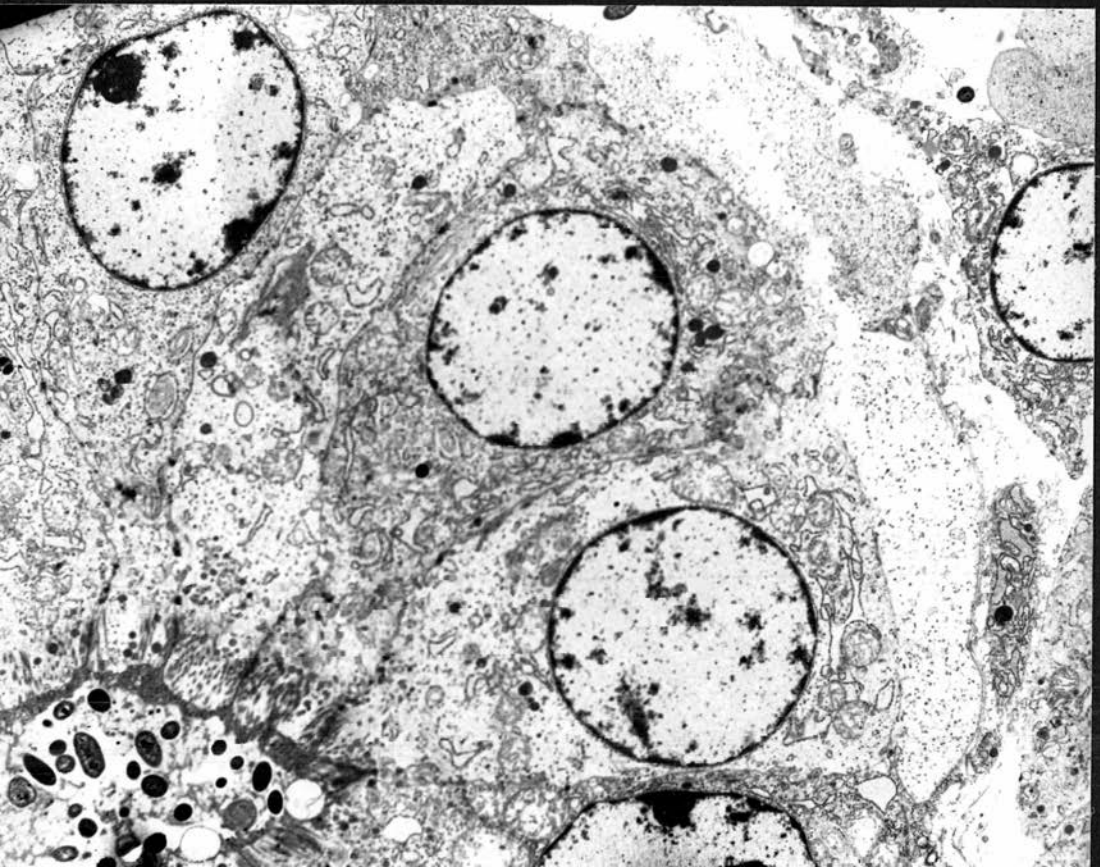

Figure 5.2. Maintenance isolator used in Experiment 1.

Figure 5.3. Electric fan and inlet air-filter.

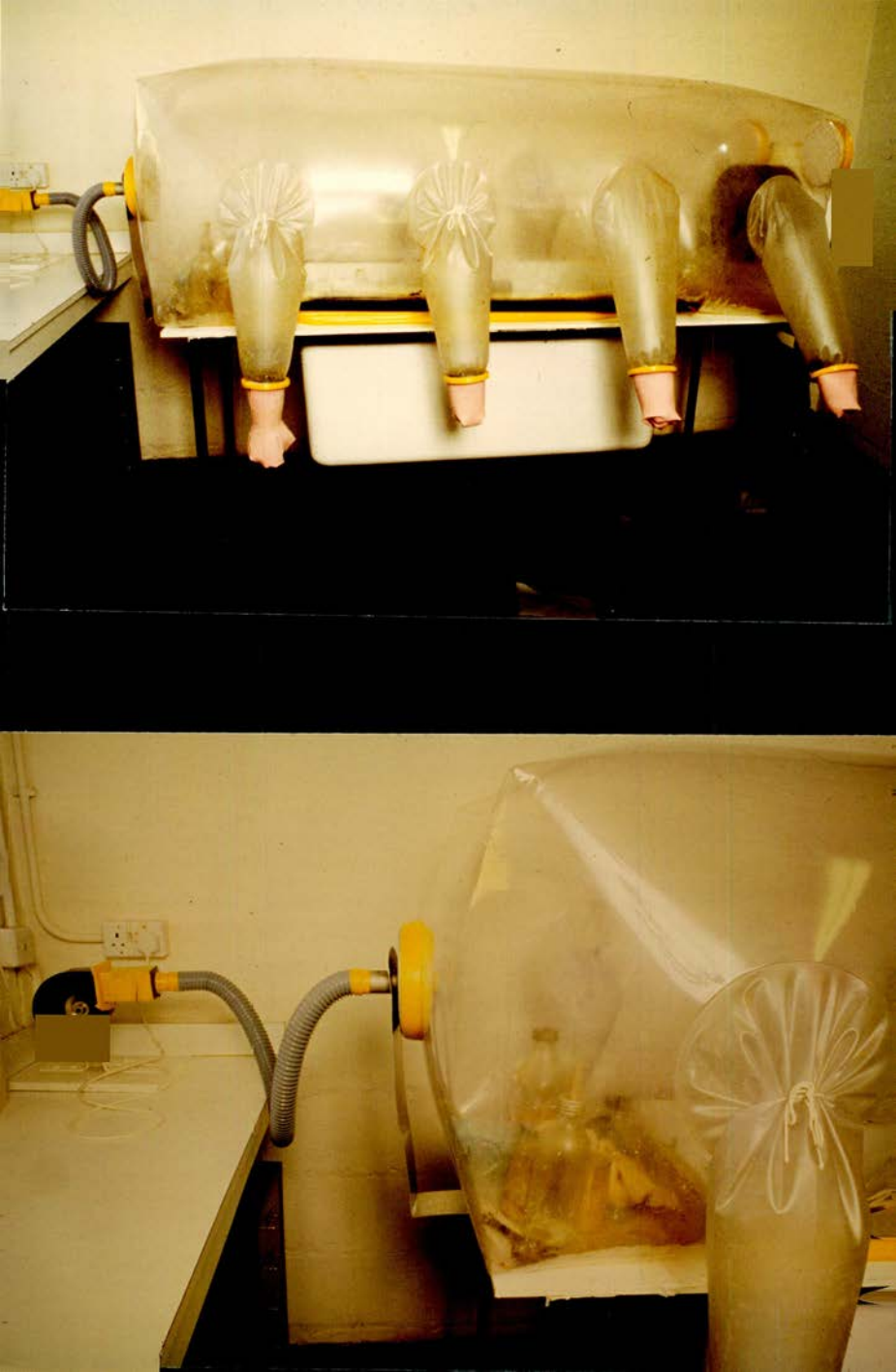

Figure 5.4. Interior of maintenance isolator, Experiment 1. Two sleeping piglets.

Figure 5.5. Entry port/disinfectant lock and exit air-filters.

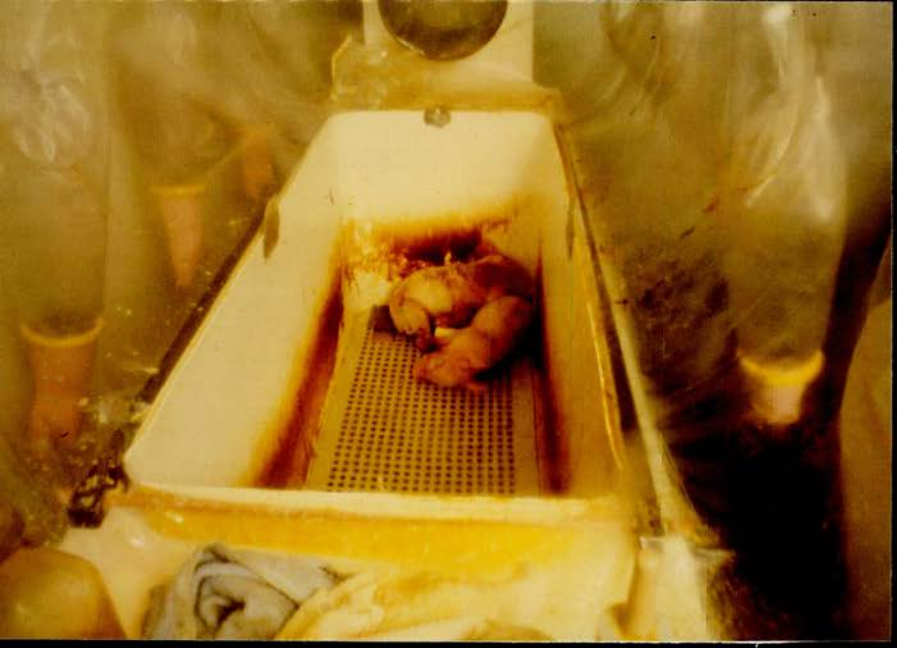

Figure 5.6. Bottle-feeding a gnotobiotic piglet.

Figure 5.8. Piglet G2, Duodenum. H. & E. x 128.

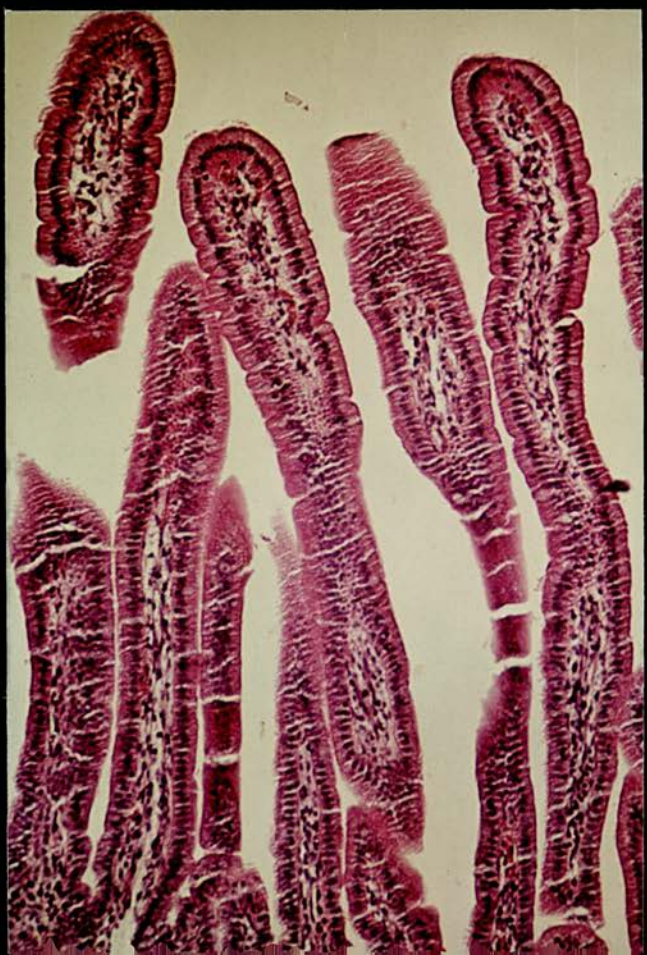

Figure 5.9. Piglet G2, MS1.
H. & E. x 128.

Figure 5.10. Piglet G2, TS1.
H. & E. x 128.

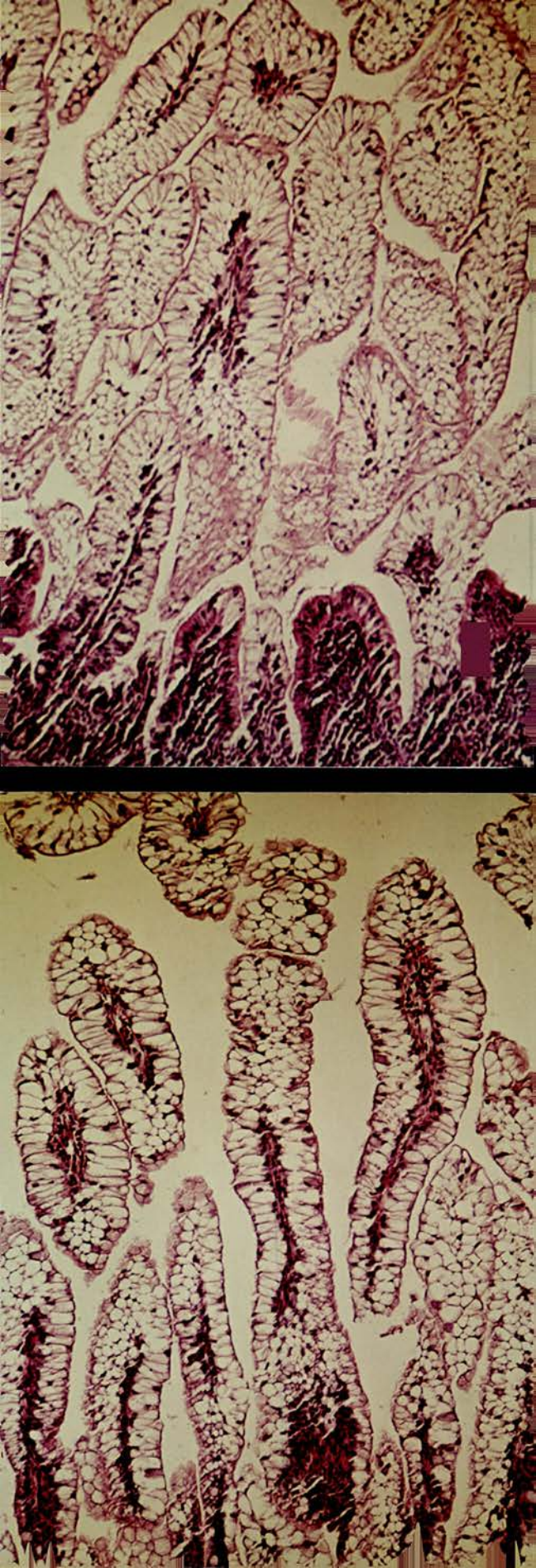

Figure 5.11. Piglet G2, Caecum.
H. & E. x 320.

Figure 5.12. Piglet G2, LB.
H. & E. x 520.

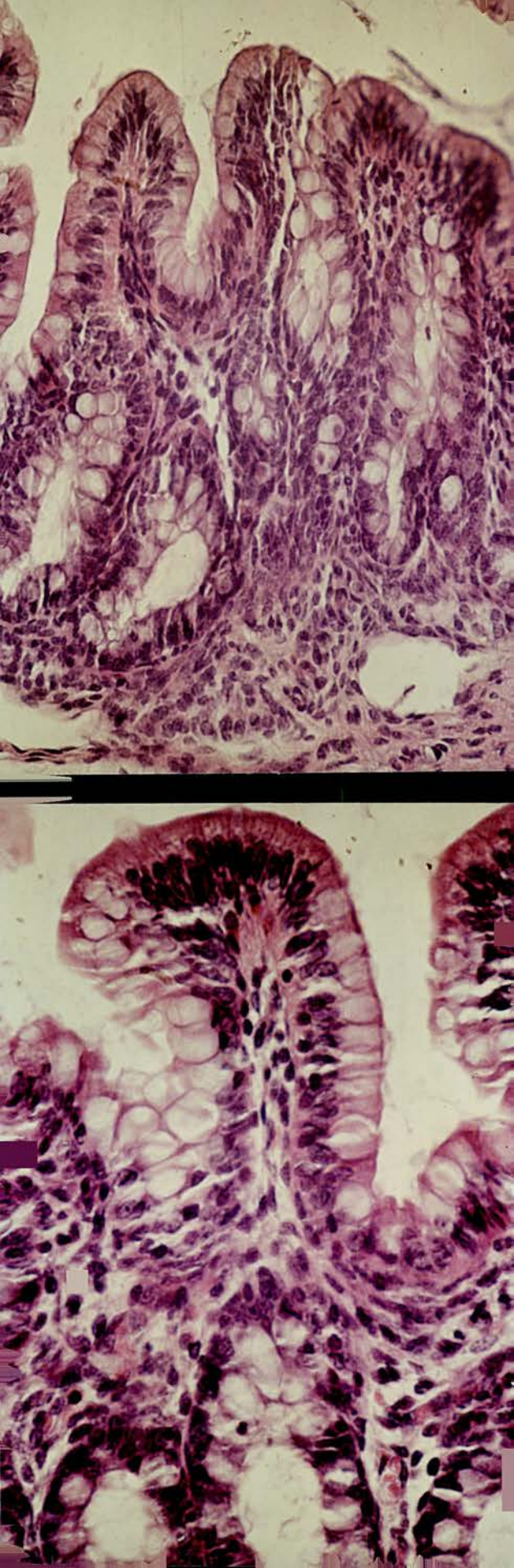

Figure 5.13. Piglet G2, TS1 Apical Tubular System. Final magnification = 53,350.

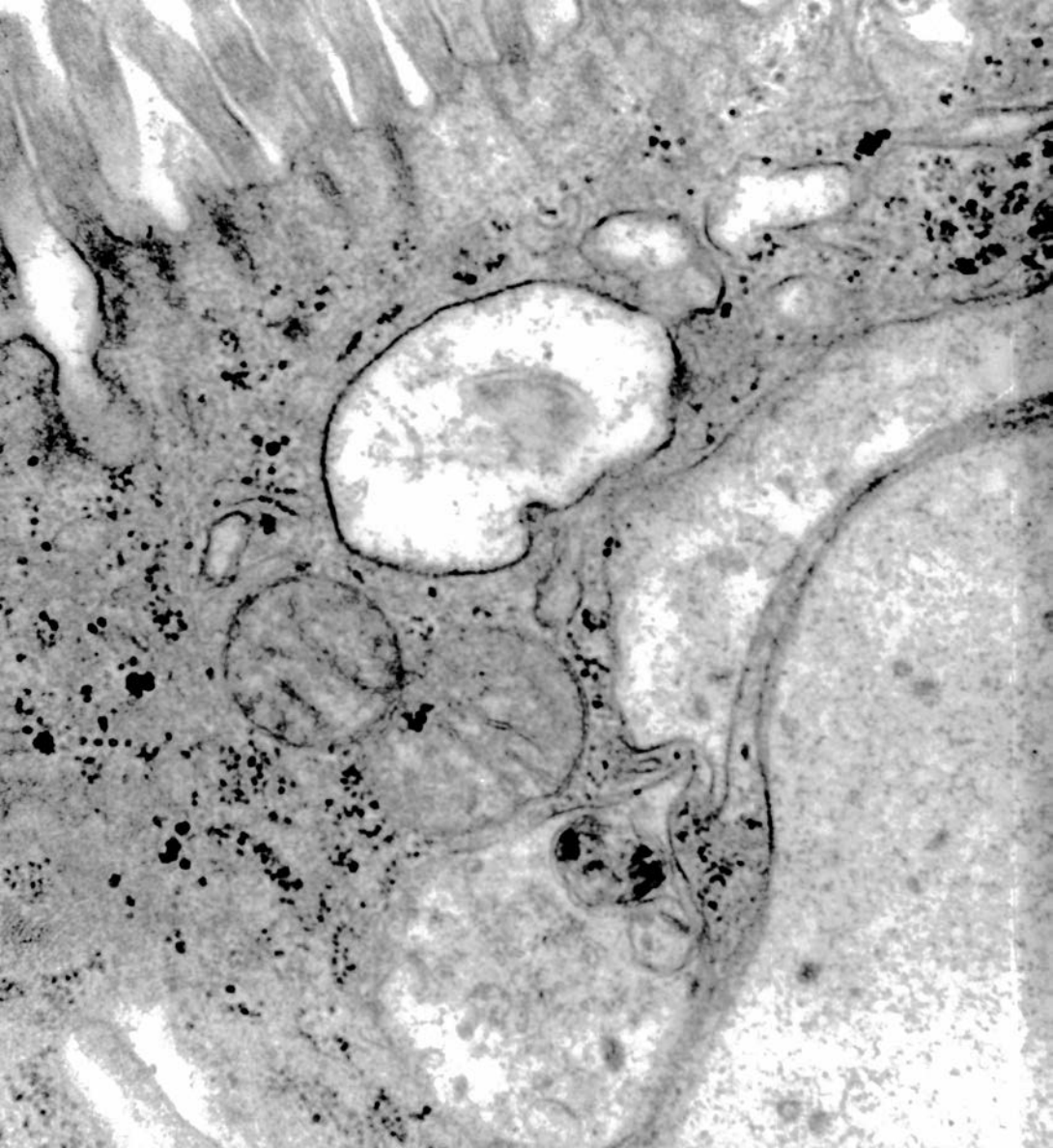

Figure 5.14. Piglet G2, TS1. Large cytoplasmic vacuoles of villar enterocytes. Final magnification = 41,500.

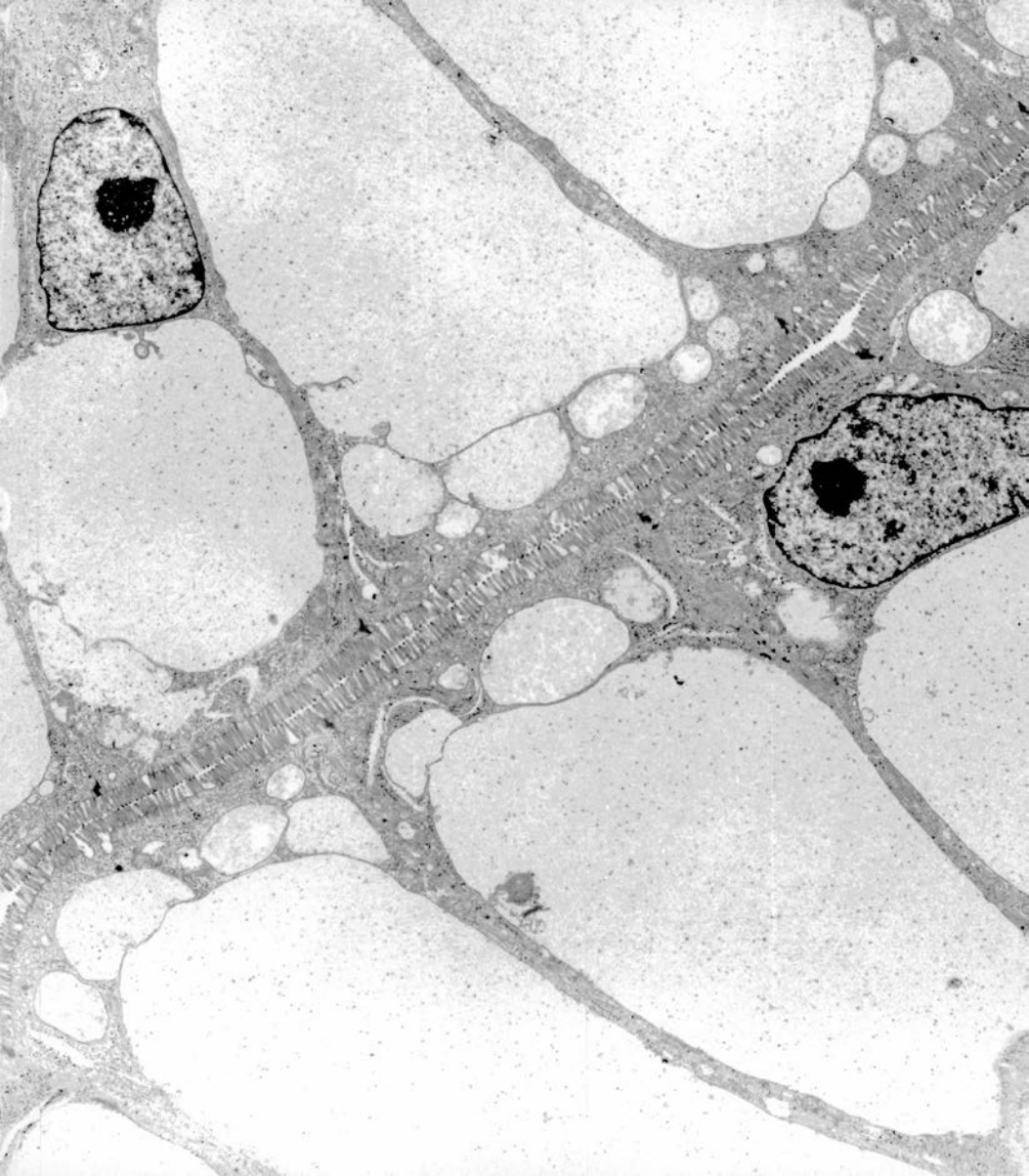

Figure 5.15. Piglet G2, TS1. Multivesicular body in apical cytoplasm. Final magnification = 53,600.

Figure 5.19. Piglet 9, Caecum and LB. Serosal oedema of large bowel and opened mucosal surface of caecum.

Figure 5.20. Piglet 9. Mucosal surface of caecum showing reddened plaque with necrotic centre. Serosal surface of spiral colon showing intense reddening and oedema.

Figure 5.21. Piglet 10, TS1. Vacuolation of villar enterocytes still present at 46 days of age. H. & E. x 320.

Figure 5.22. Piglet 9, Caecum. Relatively normal crypts in an oedematous lamina propria. Giemsa x 128.

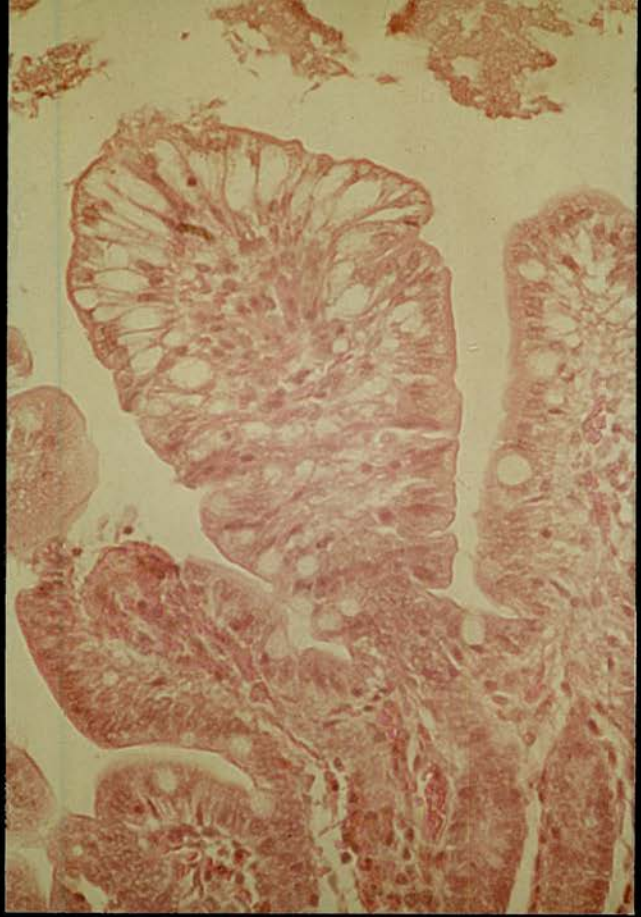

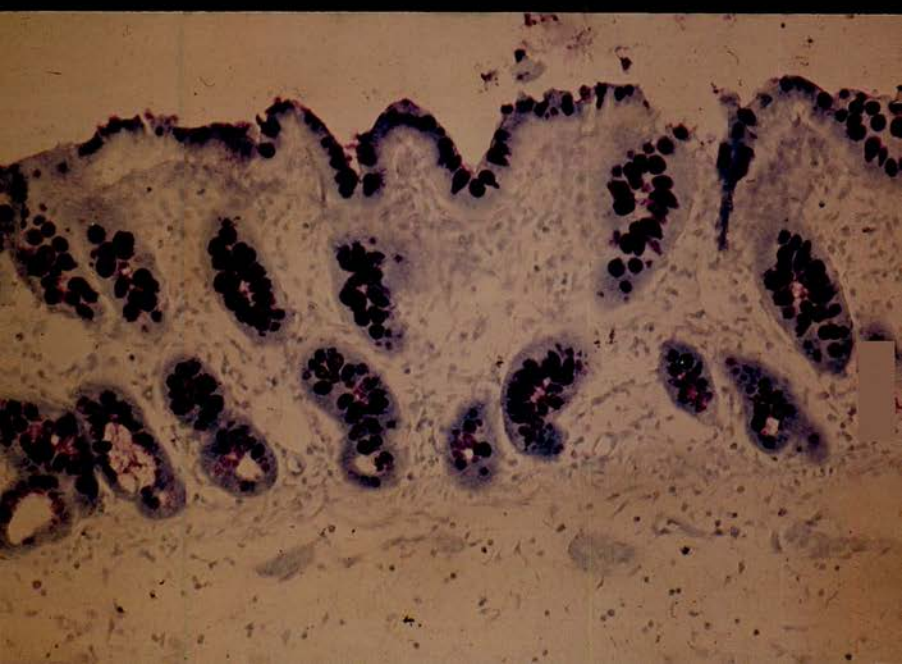

Figure 5.23. Piglet 9, Caecum. Submucosal oedema, vasculitis of submucosal vessels and moderate cellular infiltrate.
Giemsa x 64.

Figure 5.24. Piglet 9, Caecum. Submucosal vessel showing mainly eosinophilic vasculitis.
H. & E. x 600.

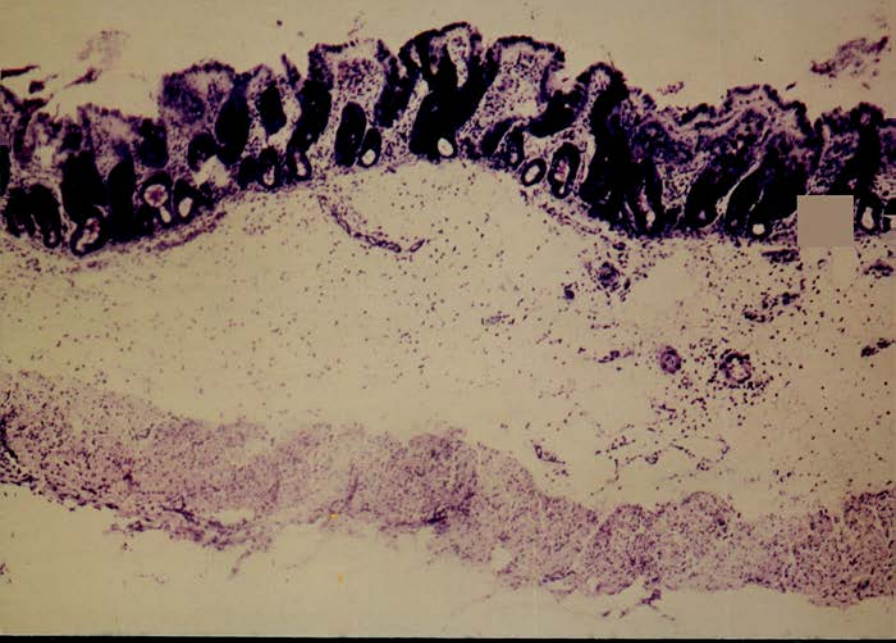

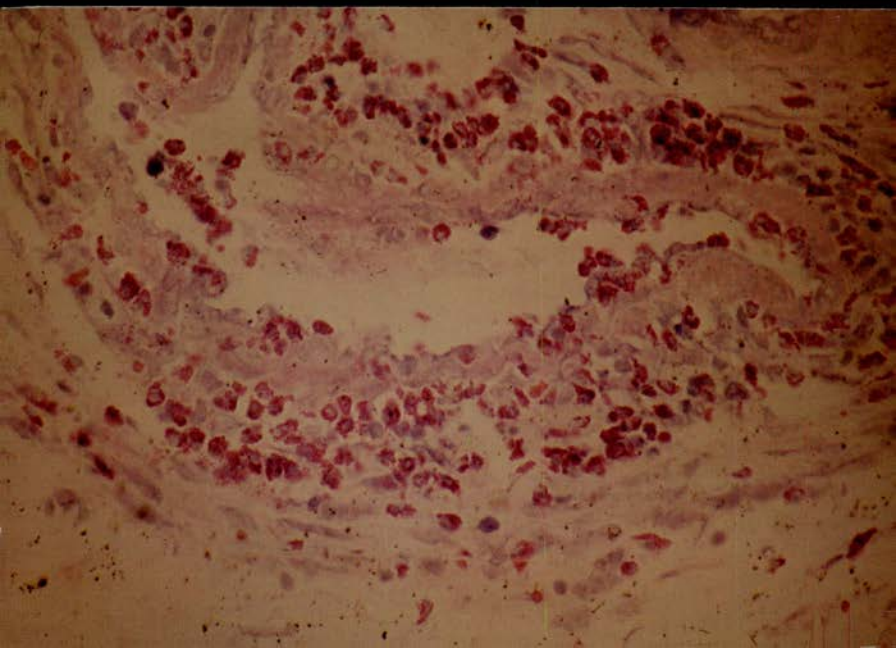

Figure 5.25. Piglet 11, TS1. Portion of villus showing large cytoplasmic vacuoles. No evidence of intracellular bacteria.
Final magnification = 5,500.

Figure 5.26. Piglet 11, Caecum. Crypt gland. Final Magnification = 5,500.

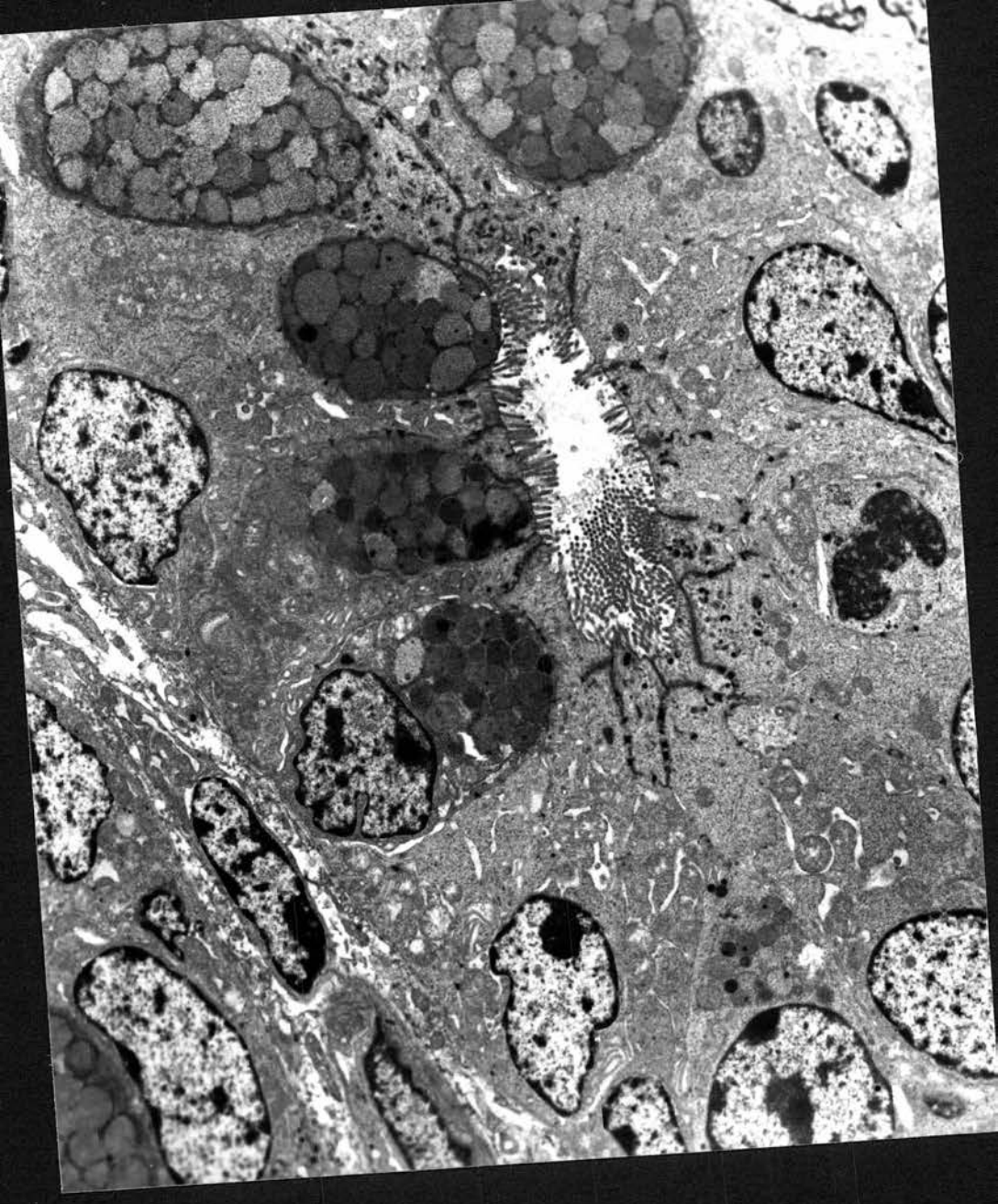

Figure 5.27. Piglet 11, TS1. *Mucosalis* bacterium lying between villi. Final magnification = 55,000.

Figure 5.28. Piglet 11, TS1. Portion of villus showing 2 tuft cells characterised by elongate microvilli.
Final magnification = 7,100.

Figure 5.29. Piglet 11, TS1. Portion of villus showing tuft cell adjacent to a vacuolated villar cell.
Final magnification = 12,000.

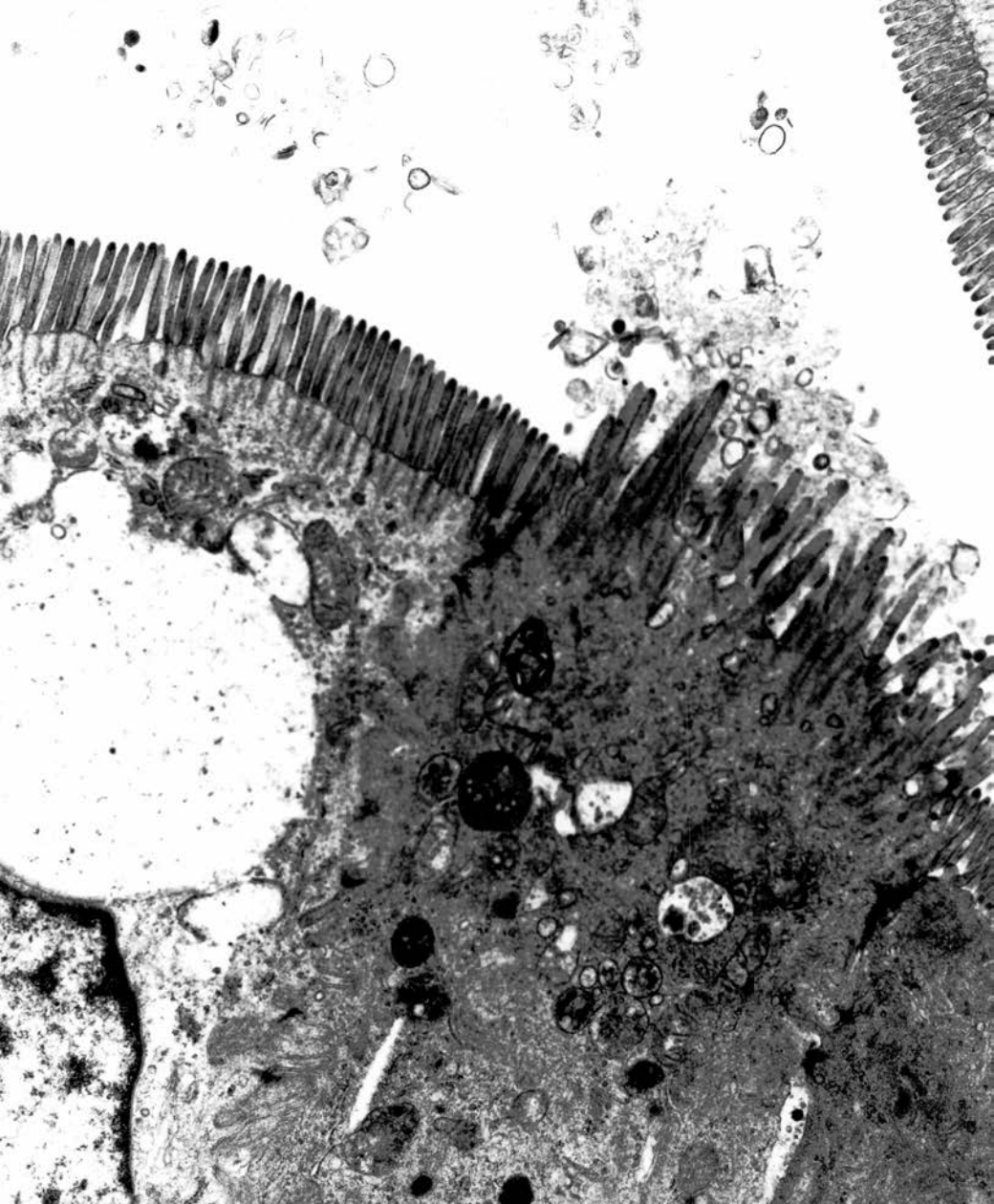

Piglet 5.30. Piglet 11, TS1. Tuft cell showing long microvilli and microvillous rootlets penetrating deep into the cytoplasm. Final magnification = 25,000.

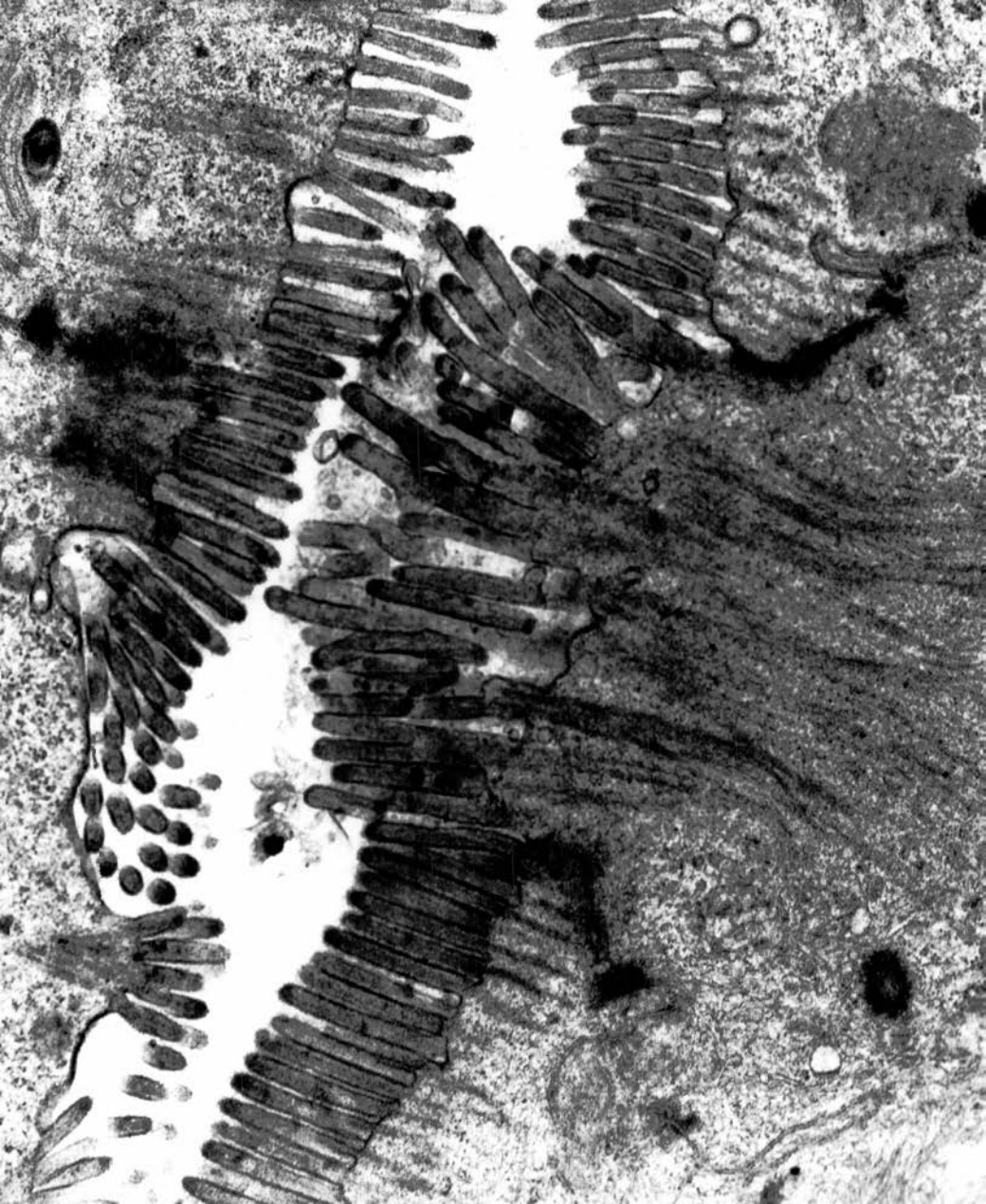

Figure 5.31. Piglet 11, TS1. Tuft cell containing supranuclear polyphagolysosome, the contents of which are similar to debris associated with the luminal mucosalis.
Cell adjacent to tuft cell contains apical bodies resembling lysosomes.
Final magnification = 15,400.

Figure 5.32. Piglet 11, TS1. Villar enterocyte showing active apical tubular system. Final magnification = 55,000.

Figure 5.33. Piglet 11, TSl. Part of crypt enterocyte. Adjacent to the nucleus is a degenerate mitochondrion containing a lamellar body of similar size and shape to mucosalis. Final magnification = 35,750.

Figure 5.34. Piglet 11, TS1. Apical cytoplasm of basal crypt gland. Numerous apical granules but no forms recognisable as mucosalis.
Final magnification = 25,000.

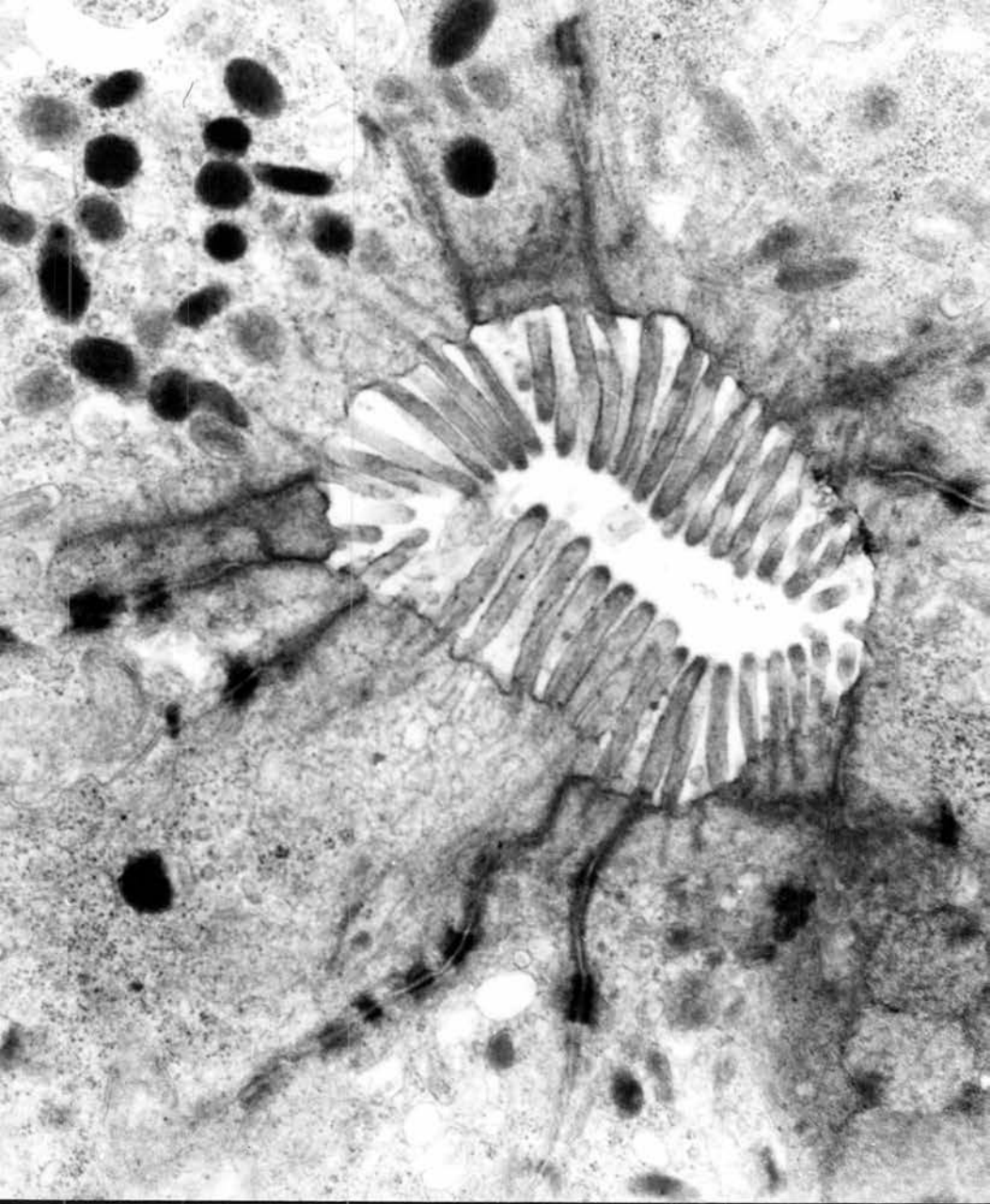

Figure 5.35. Piglet 11, TS1. Lamina propria surrounding basal crypt glands. Mucosalis free in the intercellular spaces. Note the presence of granulocytic leucocytes.
Final magnification = 9,200.

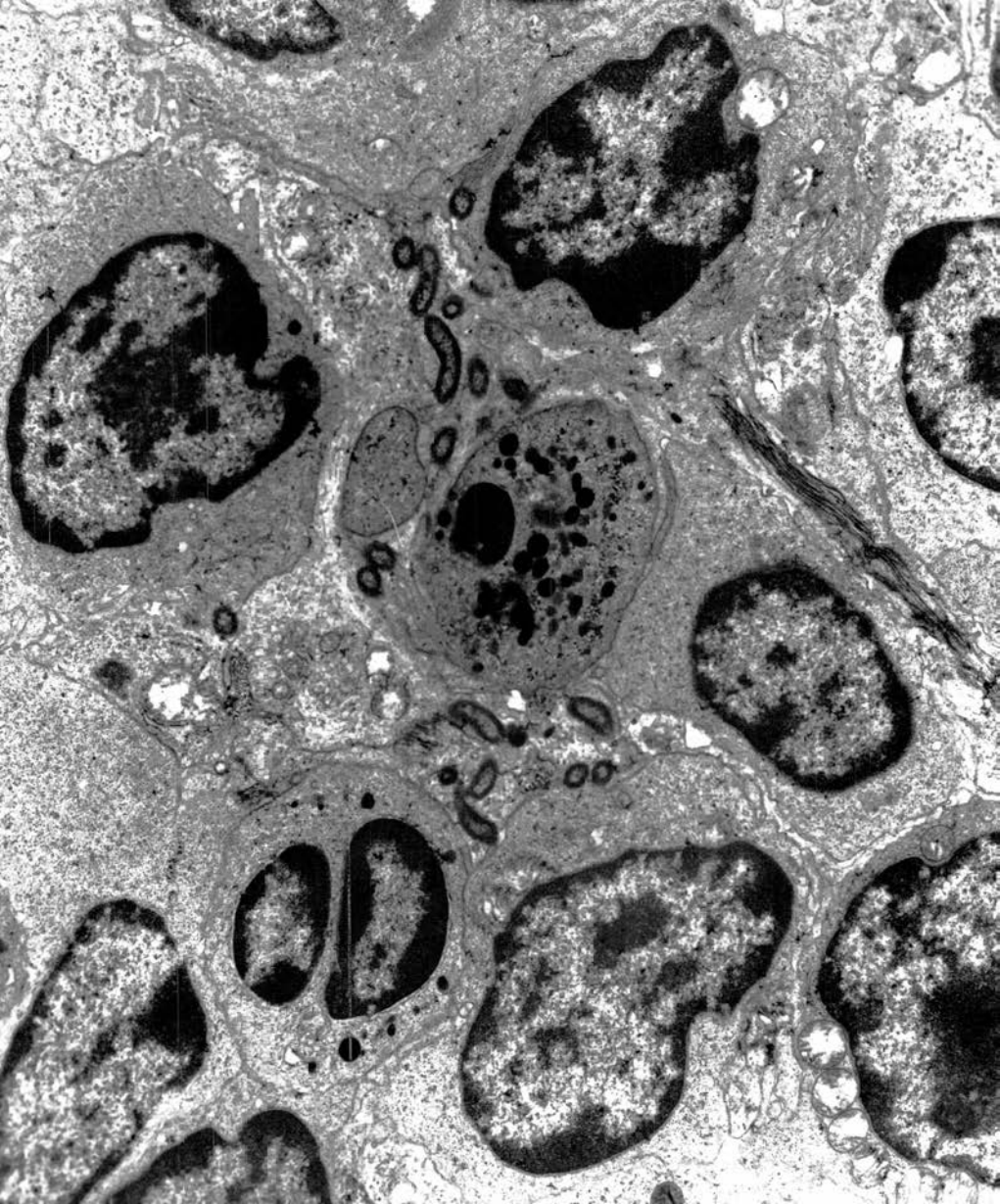

Figure 5.36. Piglet 11, TSl. Lamina propria at base of crypt gland. Several mucosalis present between the base of crypt enterocytes (upper right) and cells of the lamina propria (lower left).
Final magnification = 21,875.

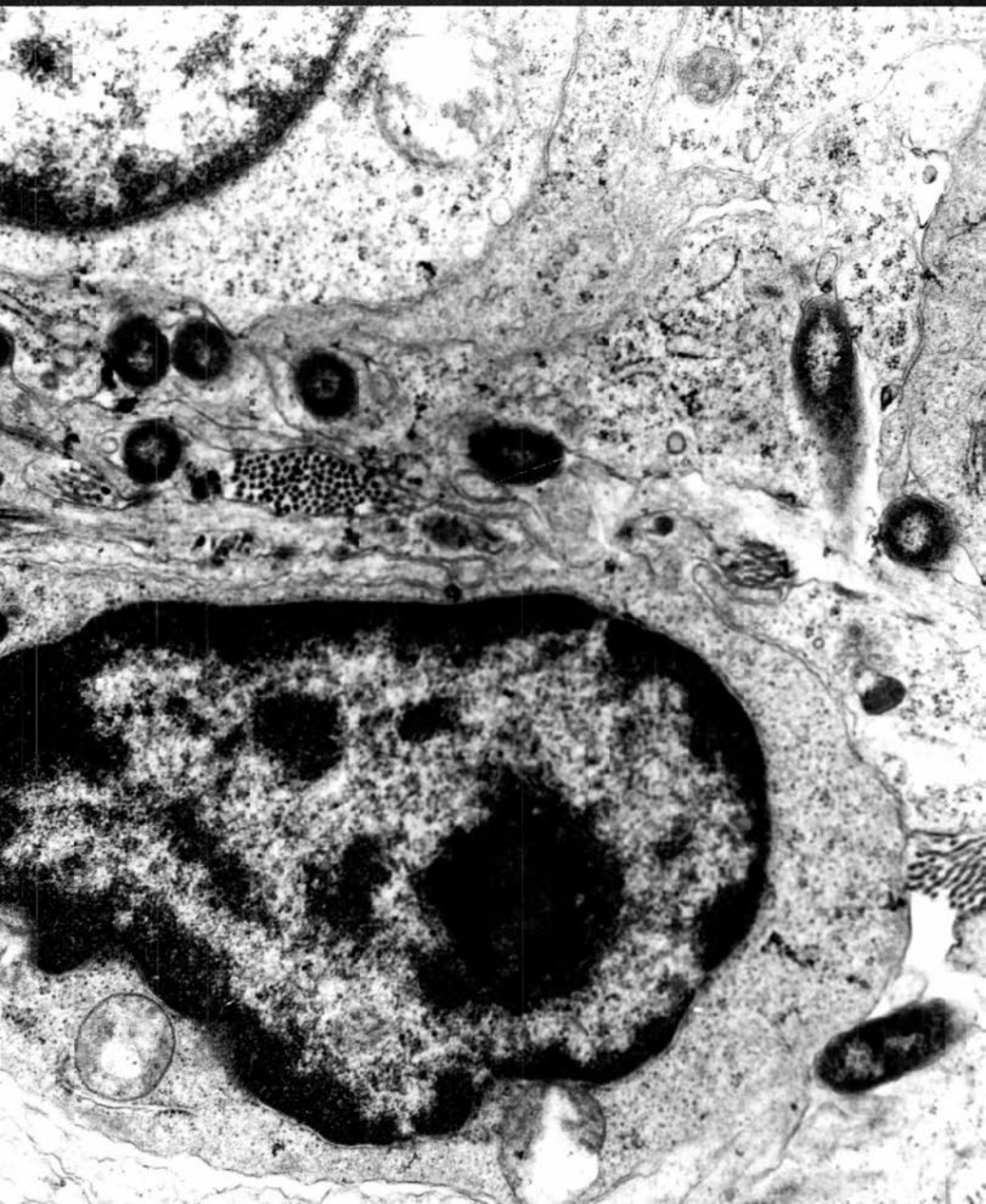

Figure 5.37. Piglet 11, TS1. Lamina propria surrounding basal crypt glands. *Mucosalis* free in the intercellular spaces. Despite proximity of granulocytic leucocytes the organisms do not appear to be within the phagocytic vacuoles.
Final magnification = 33,000.

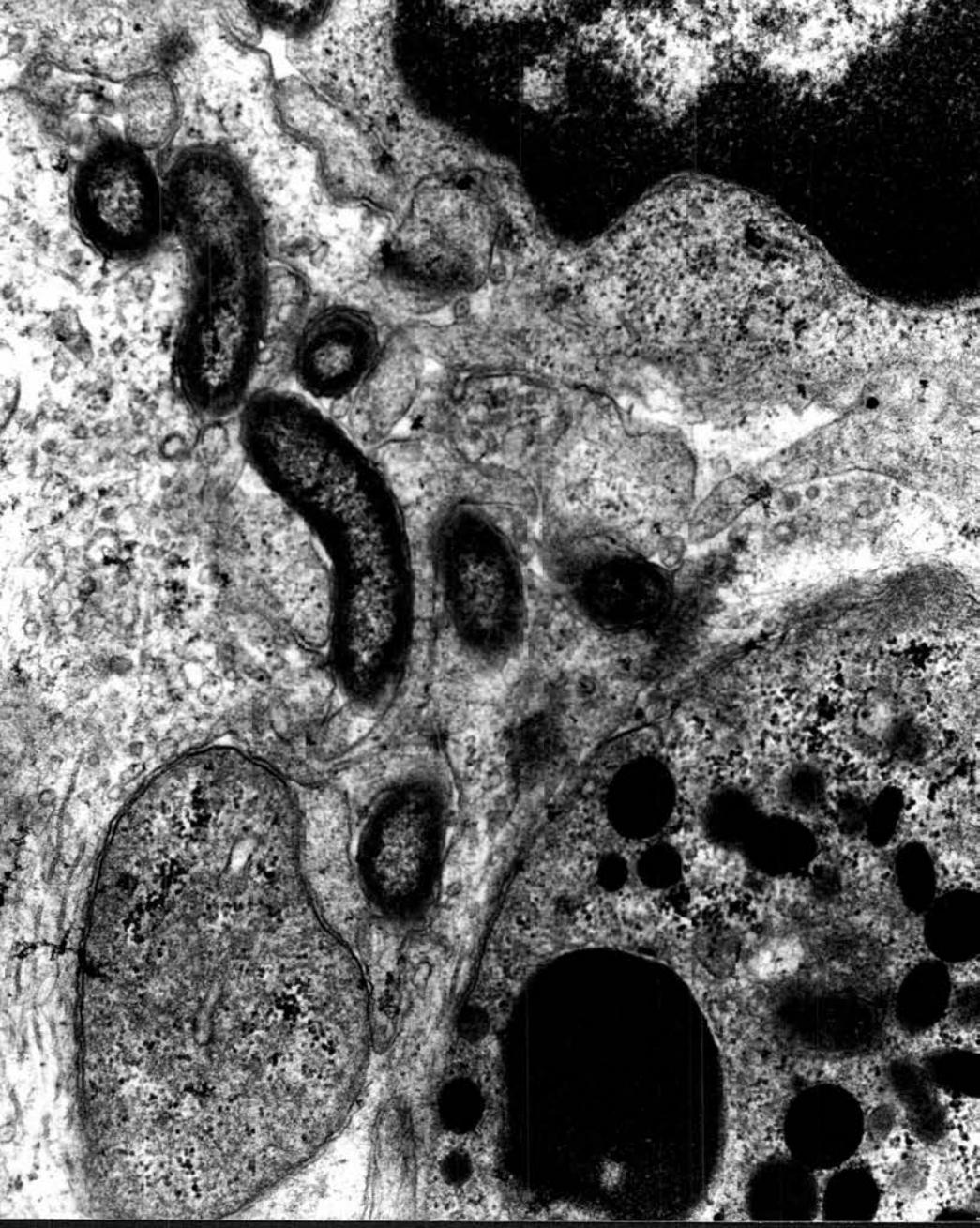

Figure 5.38. Piglet 11, TS1. High power of *mucosalis* in lamina propria. The bacteria appear morphologically typical of campylobacters and are without signs of degenerative change. Final magnification = 60,000.

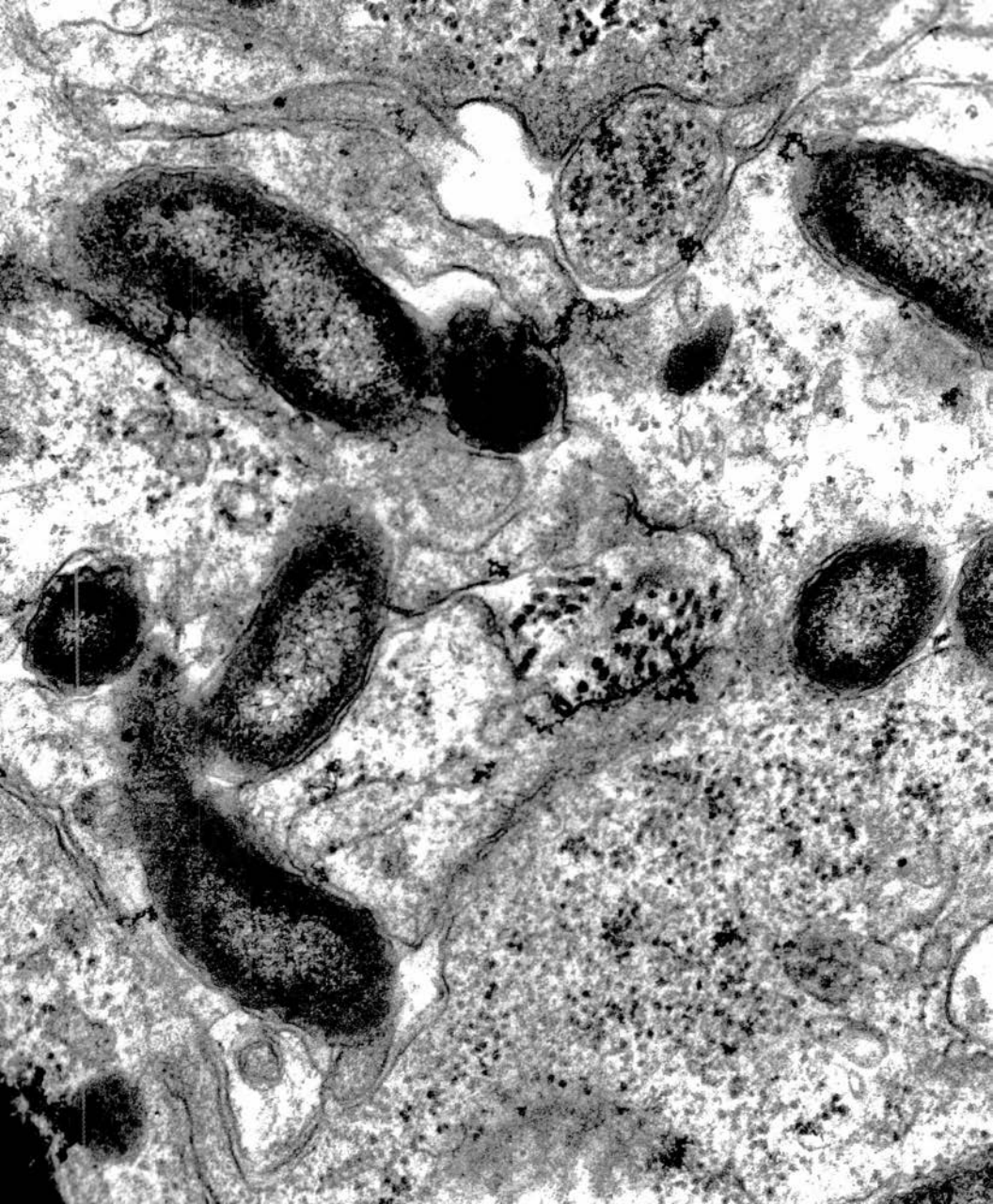

Figure 5.39. Piglet 1, LB. Luminal debris containing bacterial forms, some of which resemble campylobacters.
Final magnification = 4,300.

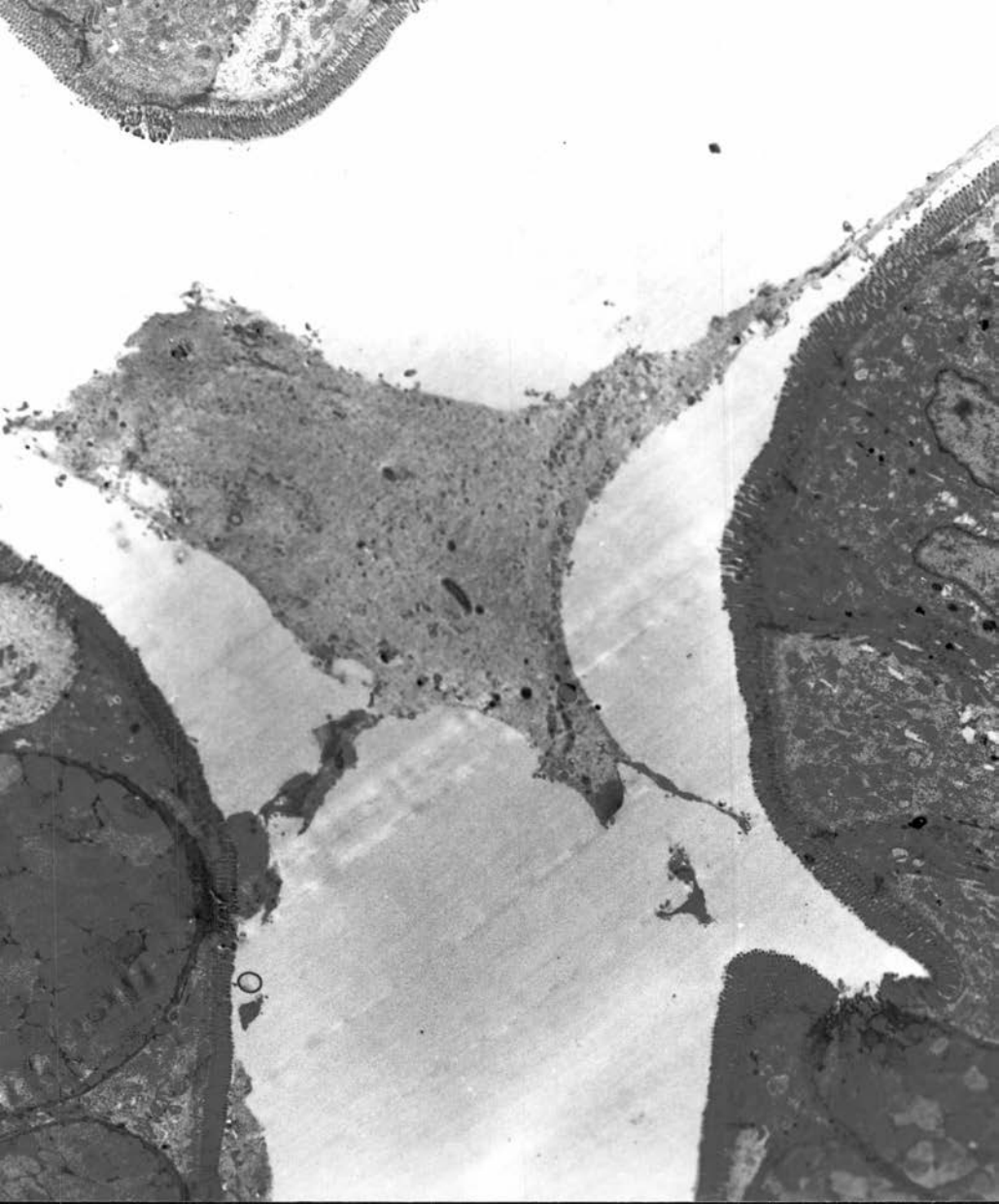

Figure 5.40. Piglet 1, LB. High power of Figure 5.39 showing one bacterium with the ultra-structural morphology of mucosalis.
Final magnification = 71,000.

Figure 5.41 Piglet 12, TS1. Immaturity of villous enterocytes demonstrated by irregular microvilli, poorly-developed apical tubular system, numerous apical granules and large numbers of free ribosomes. Final magnification = 25,000.

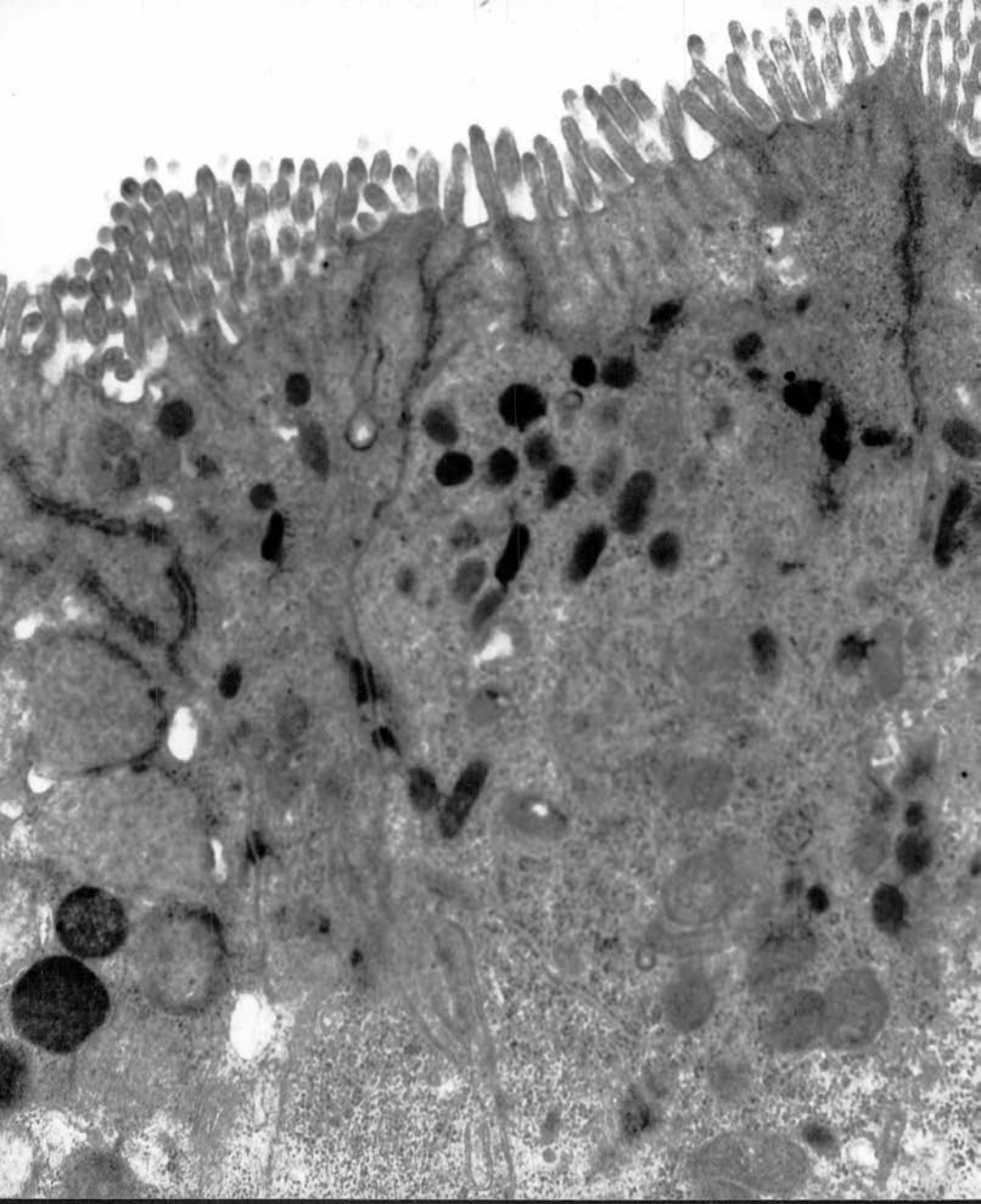

Figure 5.42. Piglet 12, MS1. Large dark-staining apoptotic mass (bottom left) in the lamina propria. Base of crypt gland just visible on the right of the picture. Final magnification = 12,000.

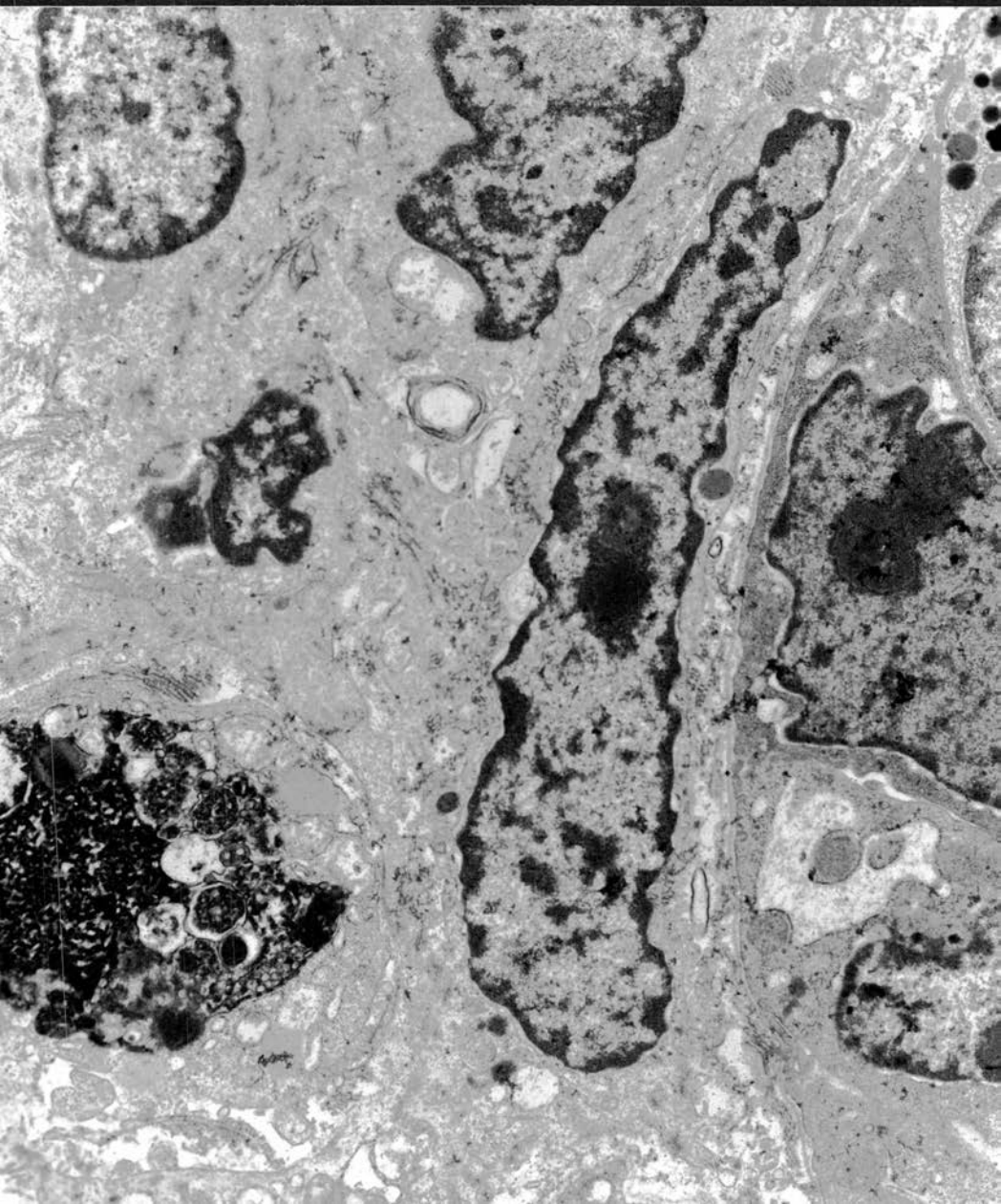

Figure 5.43. Piglet 12, MS1. High power of apoptotic mass shown in Figure 5.42.
Final magnification = 33,000.

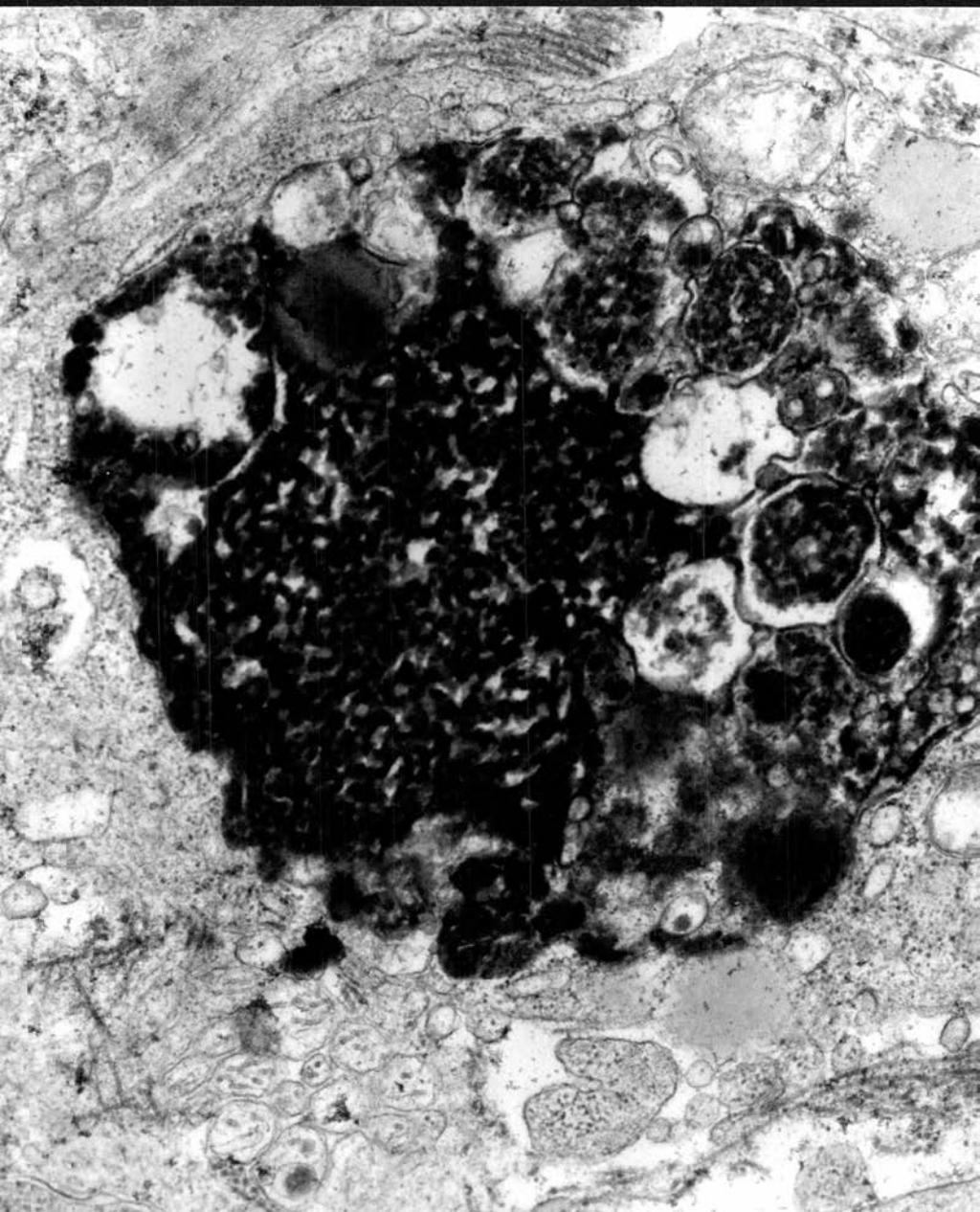

Figure 5.44. Piglet 8, LB. Mixed bacterial flora in the lumen of the spiral colon.
Final magnification = 4,300.

Figure 6.1. 987P+ *Escherichia coli*, showing pili radiating from the bacterium. Final magnification = 38,000.

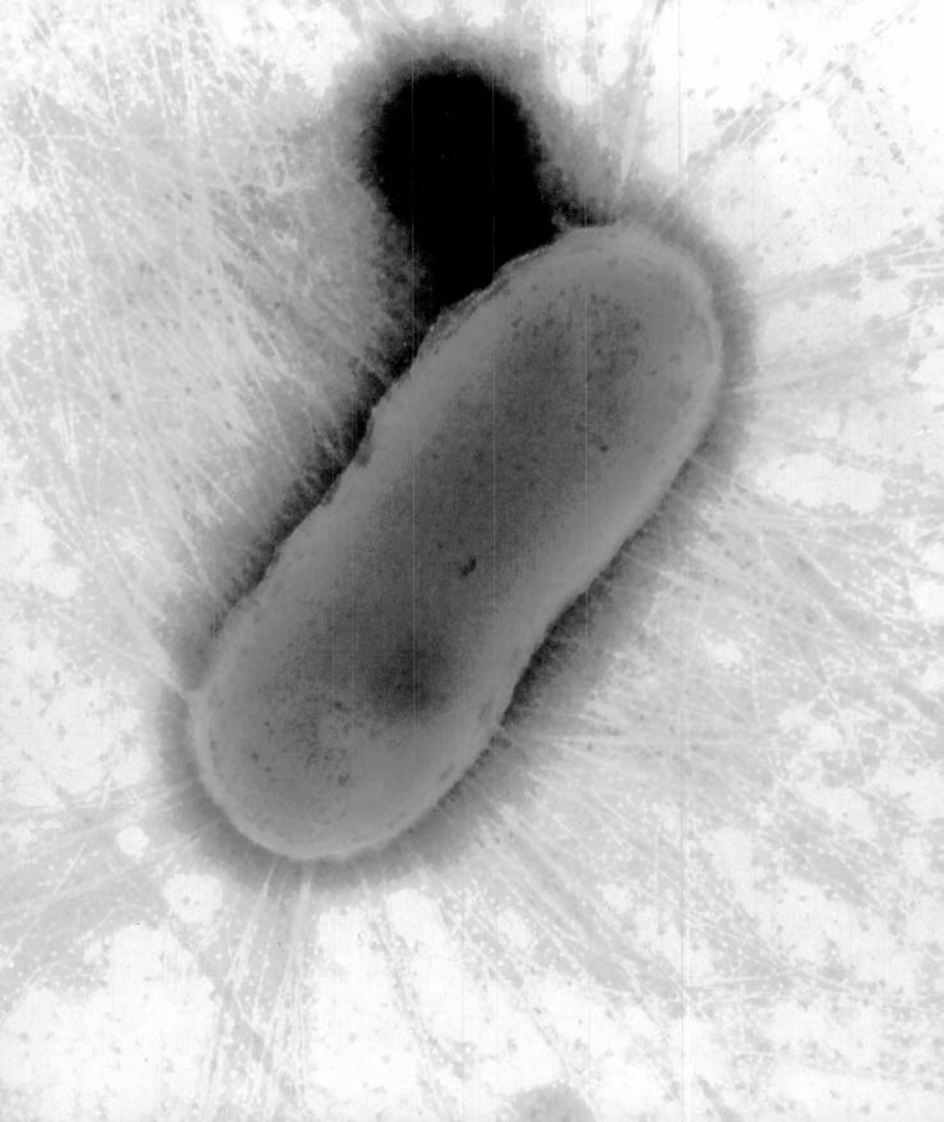

Figure 6.5. Control lamb infected with rotavirus. Tip of small intestinal villus showing bright fluorescence of cytoplasm of enterocytes. Final magnification = 500.

Figure 6.6. Piglet Y16, MSl. Tip of villus showing bright cytoplasmic fluorescence of some enterocytes. Final magnification = 500.

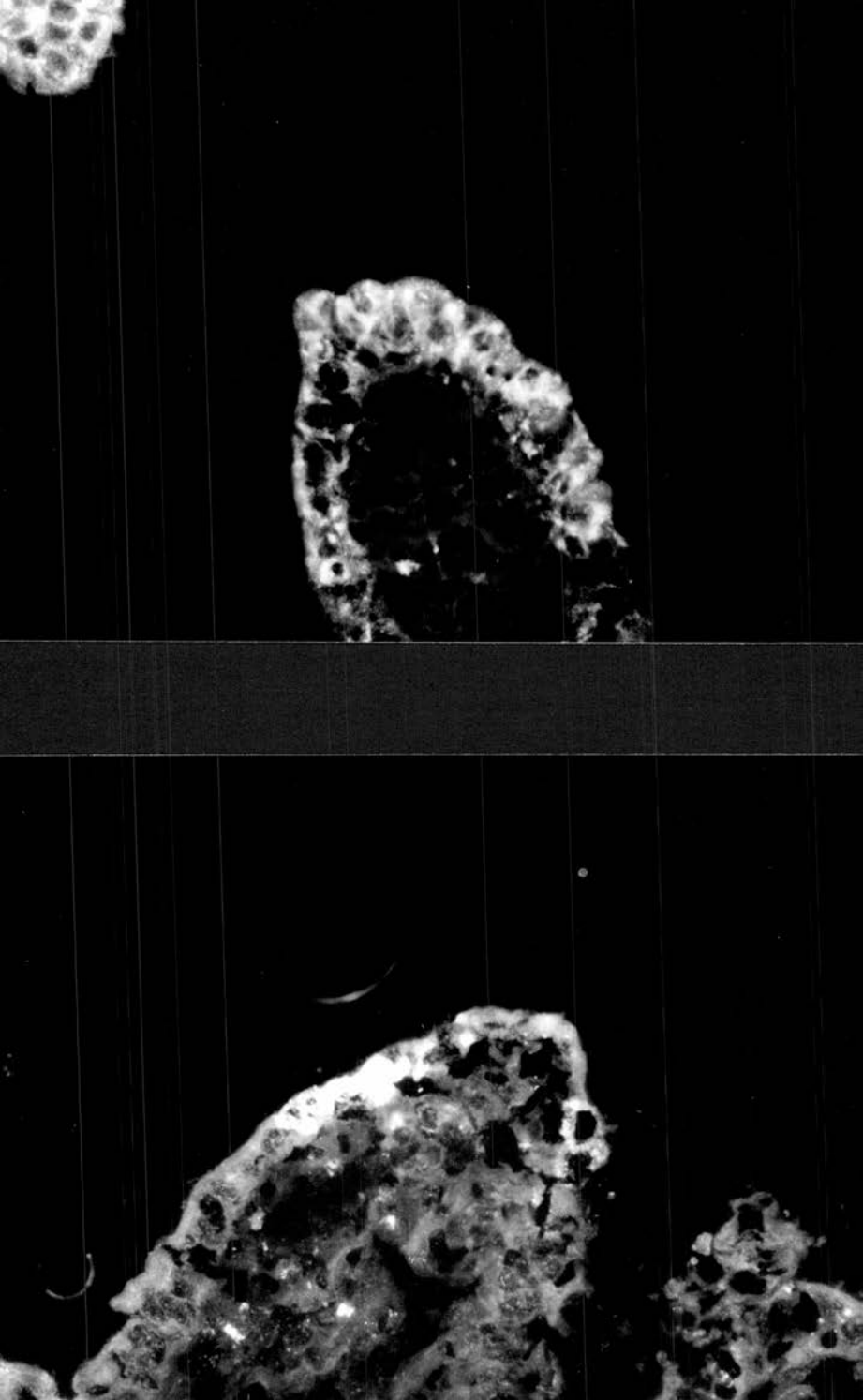

Figure 7.1. Jejunum of an SPF lamb 5 days after exposure to cryptosporidia. The area shown includes 3 stages of the life cycle of the parasite and several bacteria, possibly enterococci, adherent to the surface of host enterocytes. Final magnification = 8,000.

Figure 7.4. Piglet 185/80, TS1. Stunted villi showing heavy cryptosporidial infection as dark round bodies embedded in the brush border. Giemsa x 525.

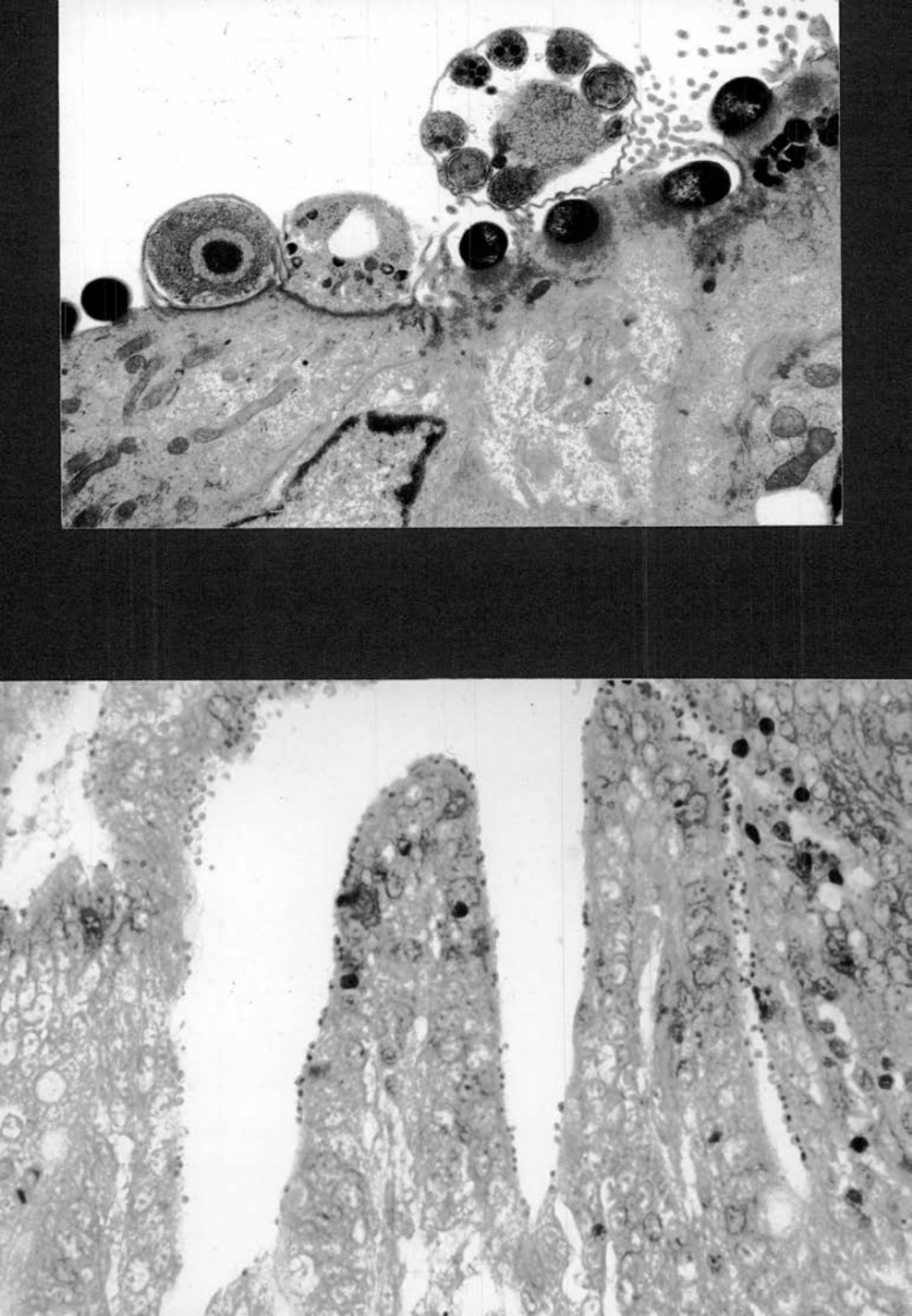

Figure 7.5. Scanning electron micrograph showing various forms of the life-cycle of cryptosporidia embedded in the microvilli of host cells.
Bar = 4μm.
Final magnification = 5,000.

Figure 7.6. Piglet 195/80, TS1. Transmission electron micrograph showing numerous cryptosporidia attached to the surface of the host enterocytes.
Final magnification = 4,125.

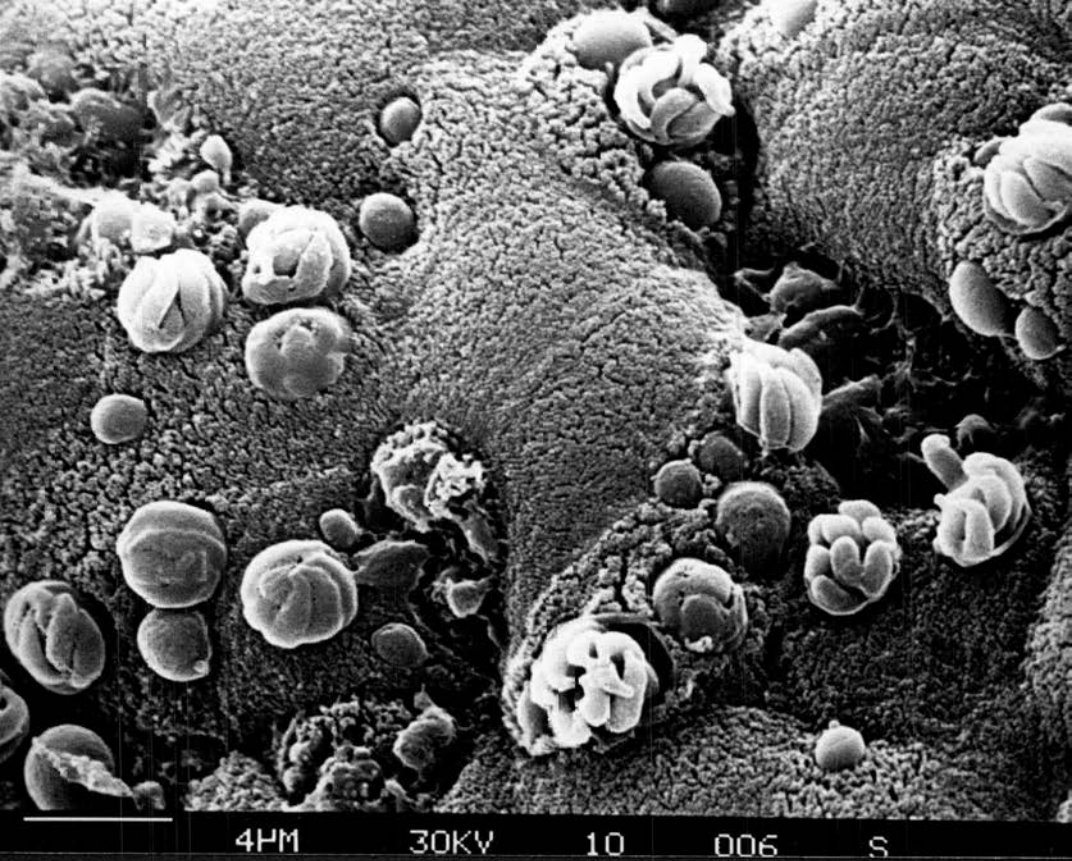
4PM 30KV 10 006 S

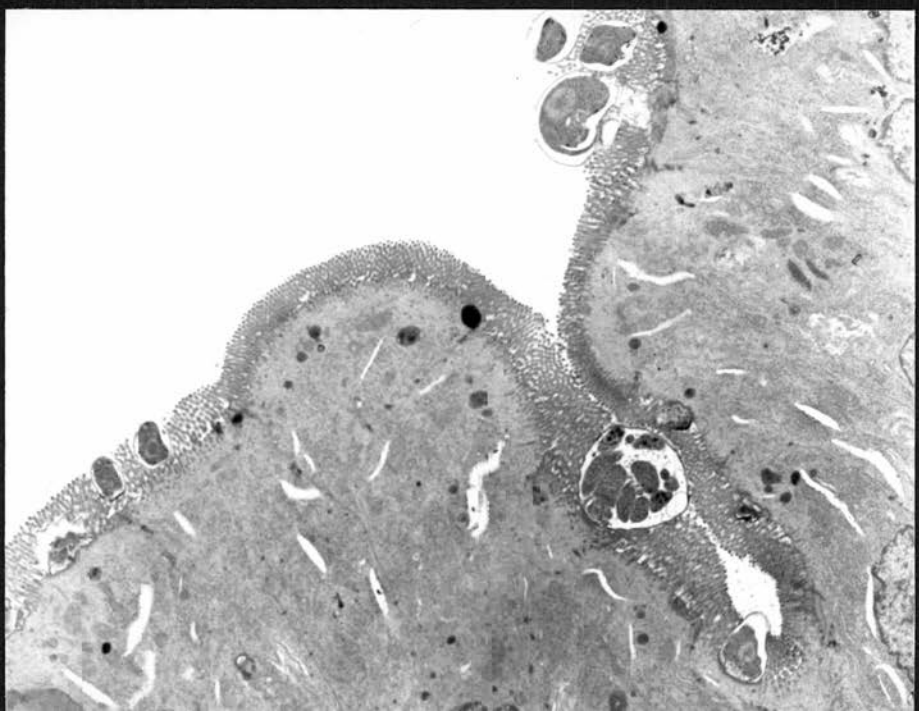

Piglet 7.7. Piglet 195/80. TS1 showing a number of adherent cryptosporidia, attenuation of host microvilli and infiltration of the epithelium by lymphocytes and inflammatory cells. Final magnification = 4,300.

Piglet 7.8. Piglet 185/80. TS1 showing heavy cryptosporidial infection as round basophilic bodies dotted along the surface of epithelial cells and extending to the base of crypts. Giemsa x 360.

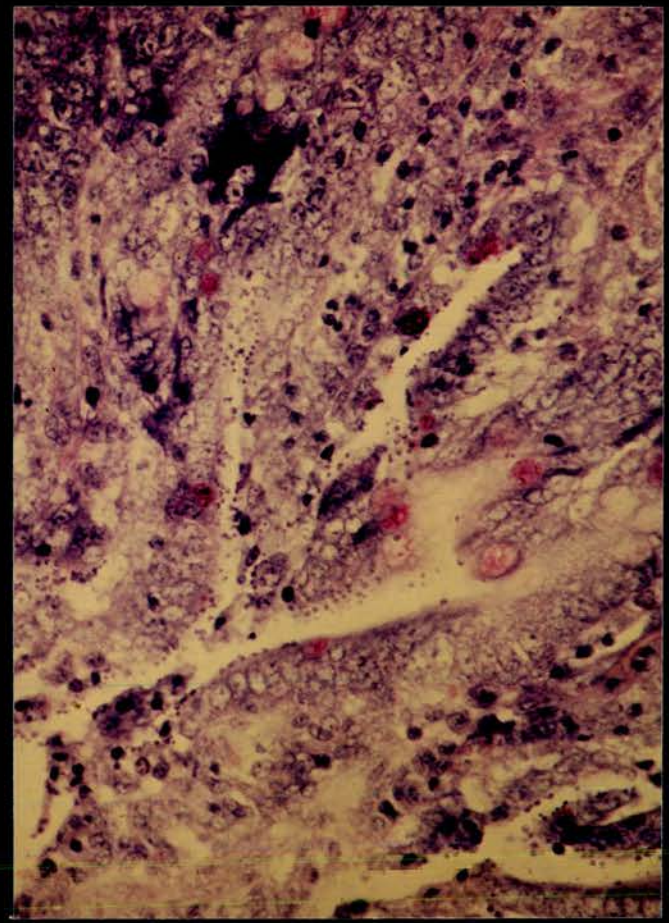

Figure 7.9. Piglet 185/80. Caecum showing cryptosporidia in the brush border of surface cells and also deeper in the crypts.
Giemsa x 900.

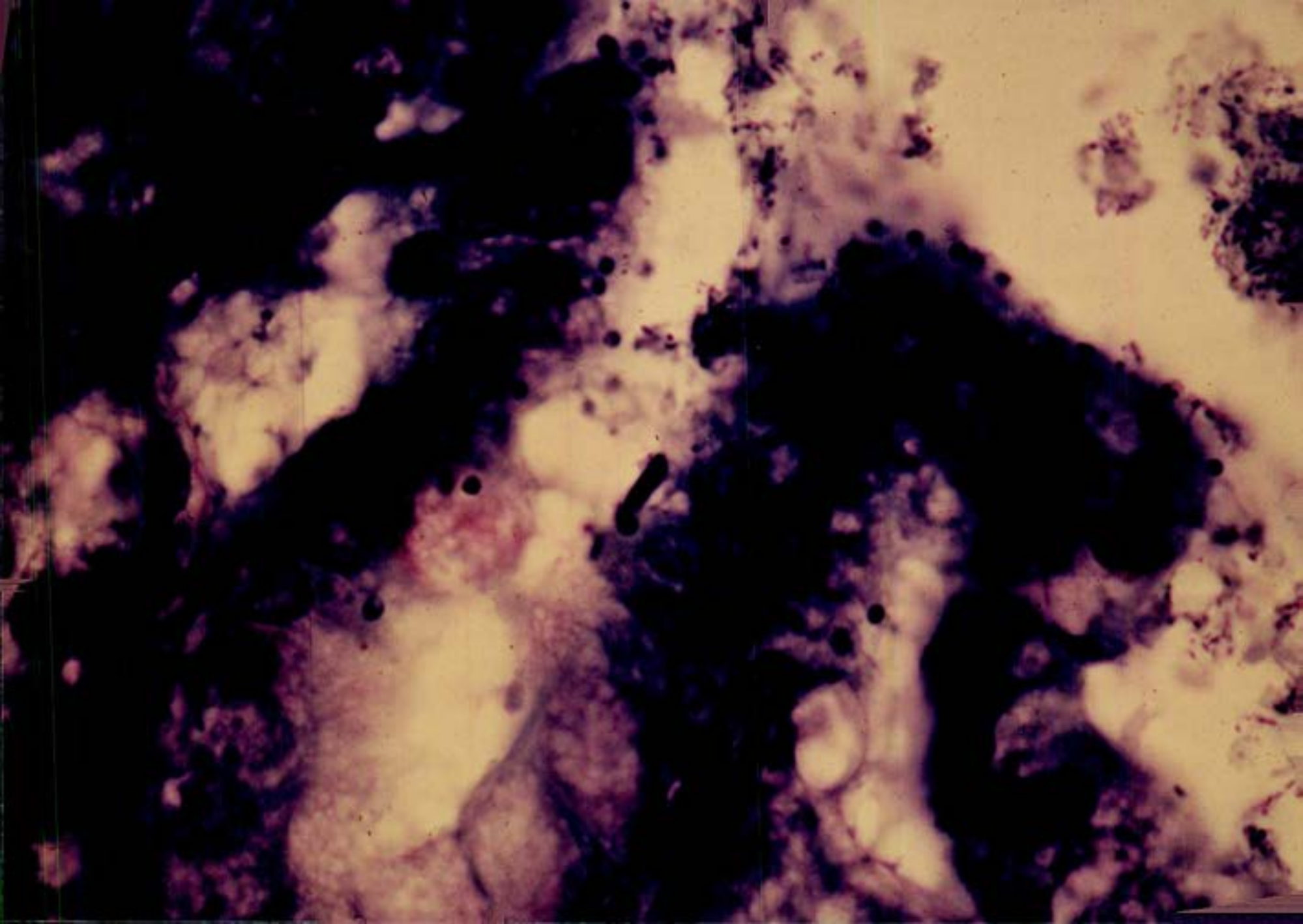

Figure 7.10. Scanning electron micrograph showing stunting and fusion of villi in the small intestine (site 4) of a cryptosporidial - exposed piglet (195/80). Compare with Figure 7.11.
Bar = 100 μm.
Final magnification = 200.

Figure 7.11. Scanning electron micrograph showing normal villi in the small intestine (site 4) of a control piglet (194/80). Compare with Figure 7.10.
Bar = 100 μm.
Final magnification = 200.

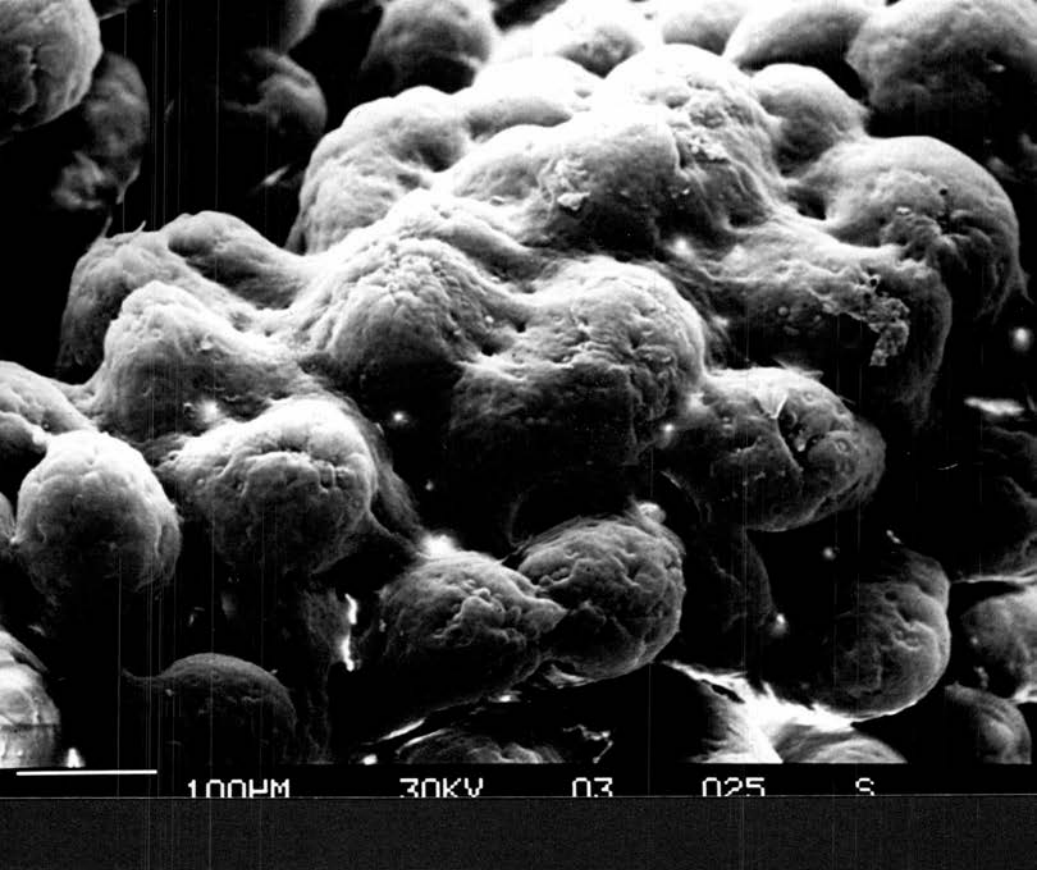
100UM 30KV 03 025 S

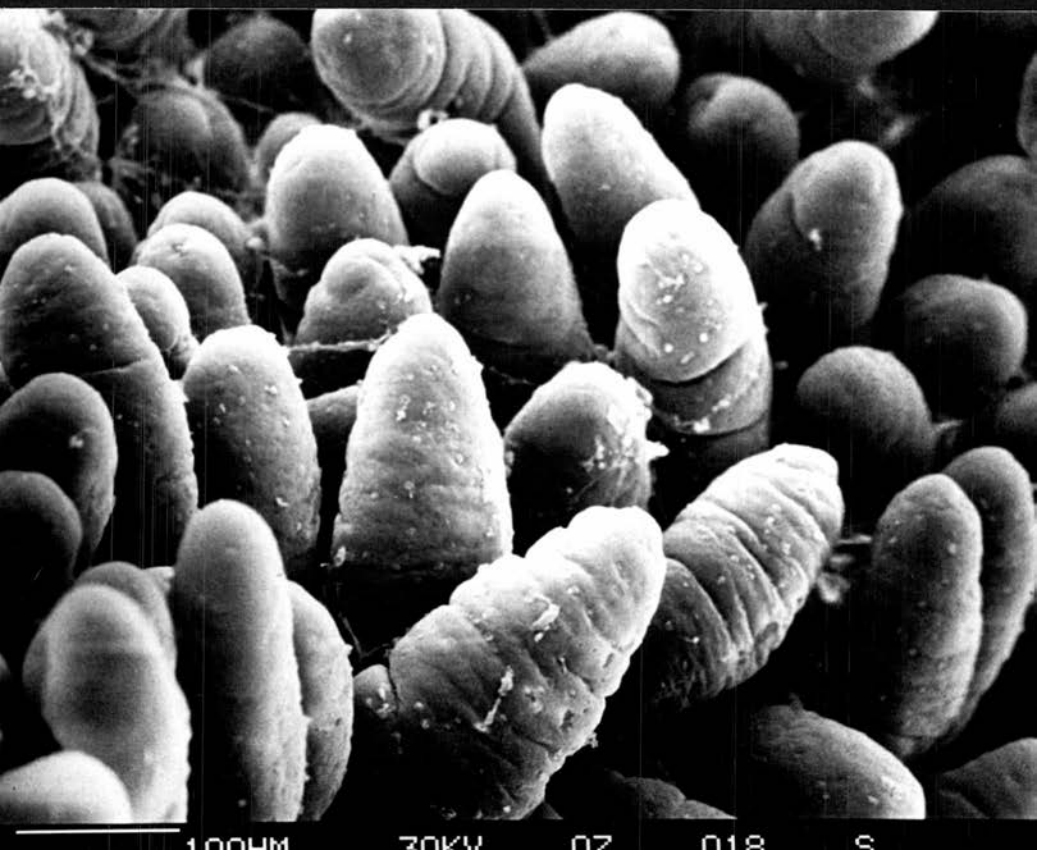
100UM 30KV 07 018 S

Figure 7.12. Piglet 185/80, site 4. There is severe stunting and fusion of villi associated with heavy cryptosporidial infection.
Giemsa x 550.

Figure 7.13. Piglet 185/80, TS1. There is sloughing of the villi accompanied by an outpouring of inflammatory cells.
H. & E. x 150.

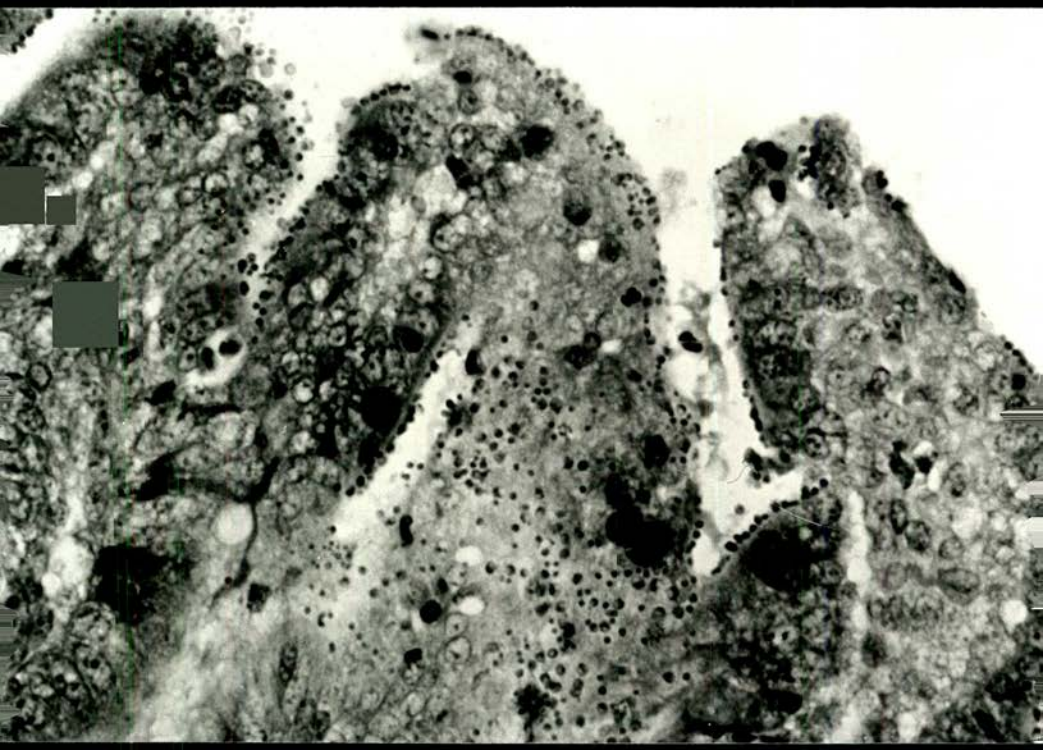

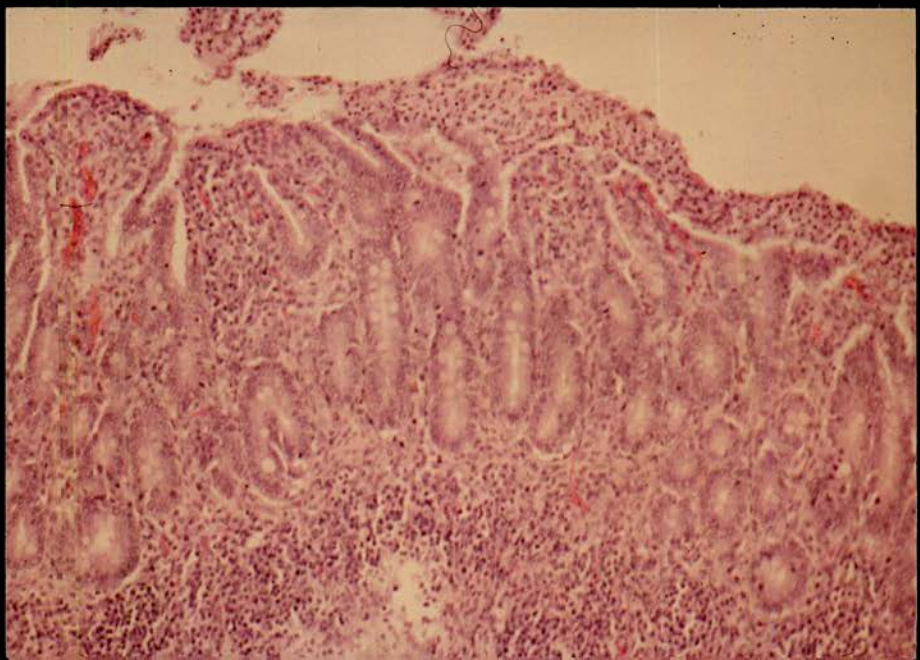

Figure 7.14. Piglet 185/80, TS1. High power showing heavy cryptosporidial infection associated with the inflammatory cell exudate. Giemsa x 375.

Figure 7.15. Piglet 195/80, TS1. Patchy areas of bacterial adherence to the villi and light cryptosporidial infection. Toluidine blue x 465.

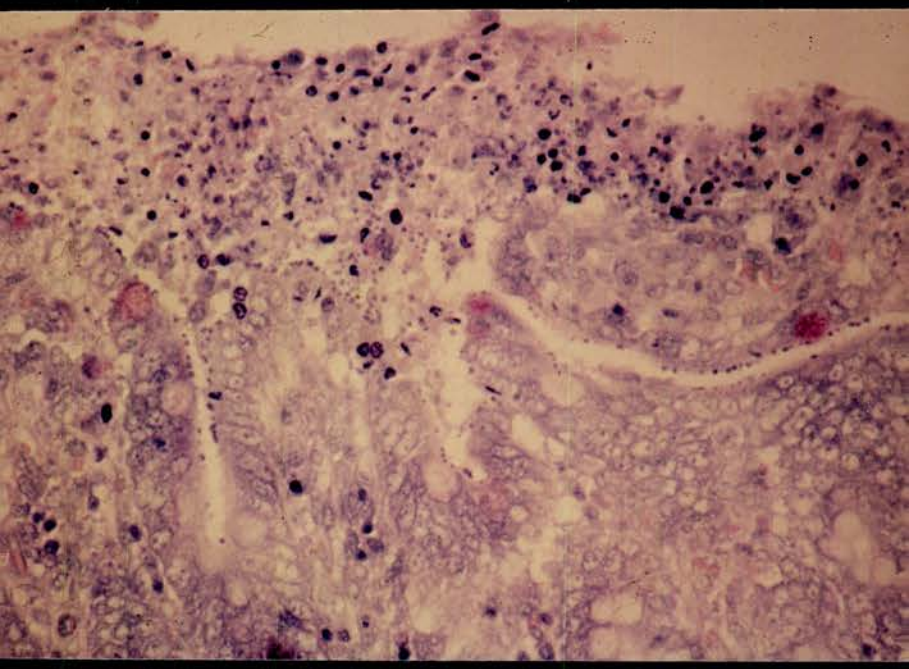

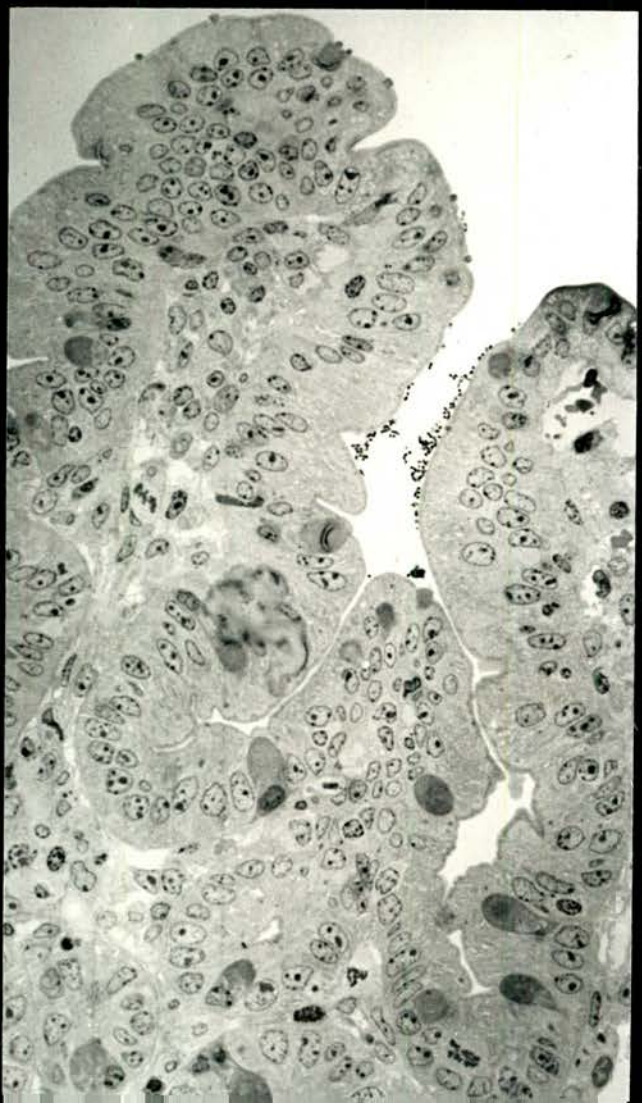

Figure 7.16. High power of Figure 7.15 showing mixed bacterial flora closely associated with the surface of host enterocytes.
Toluidine blue x 1,860.

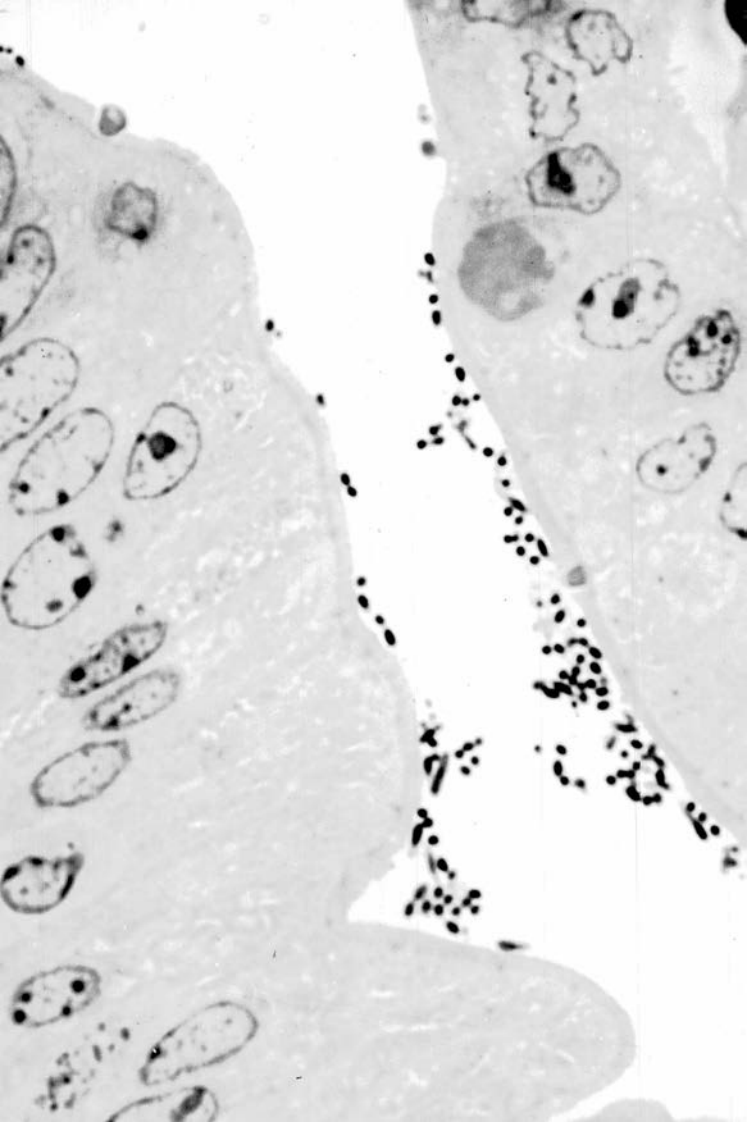

Figure 7.17. Piglet 198/80, site 4.
Scanning electron micrograph
showing adherent debris to
damaged mucosal surface.
Bar = 100μm.
Final magnification = 200.

Figure 7.18. Piglet 198/80, TS1. Transmission
electron micrograph showing
mixed bacterial flora in close
association with the surface
of villar enterocytes.
Final magnification = 5,175.

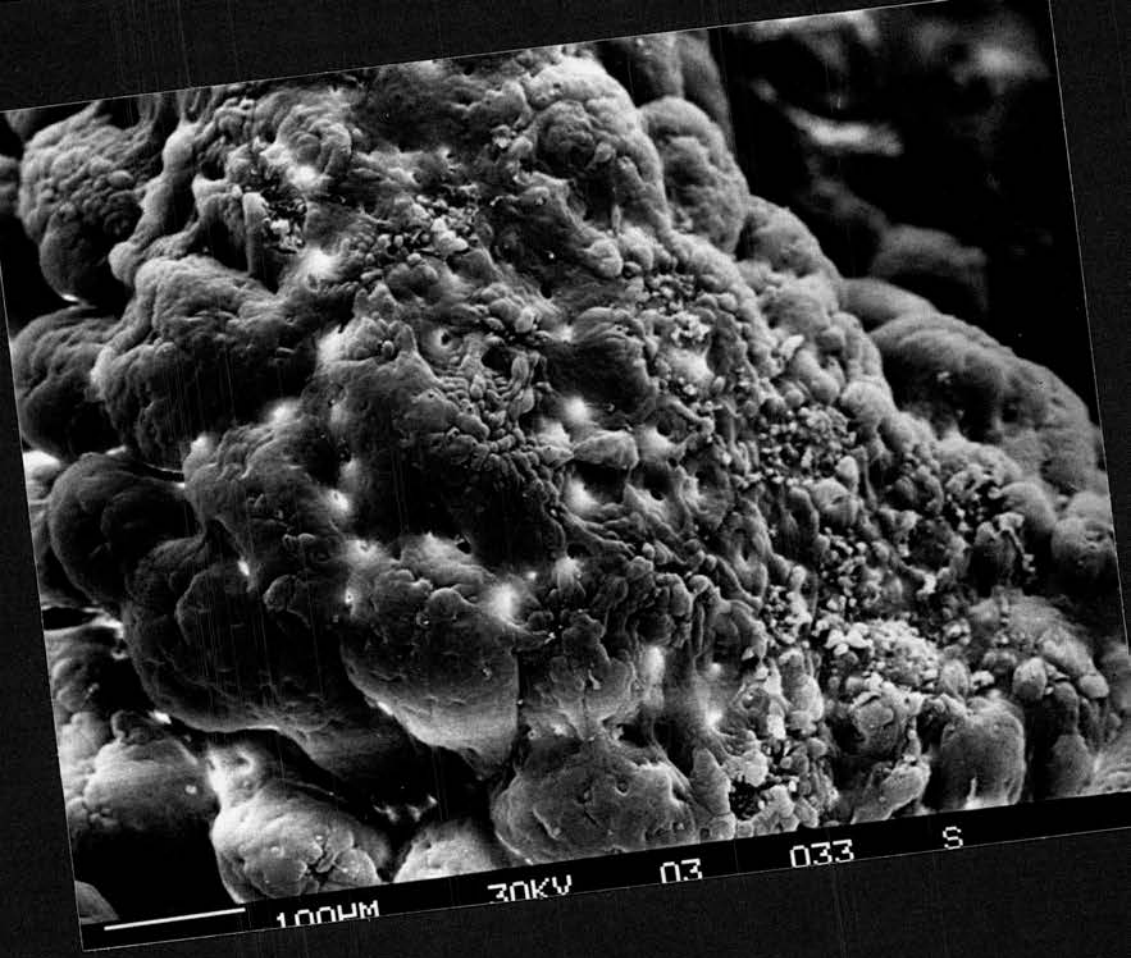
1.00UM
30kV
03
033
S

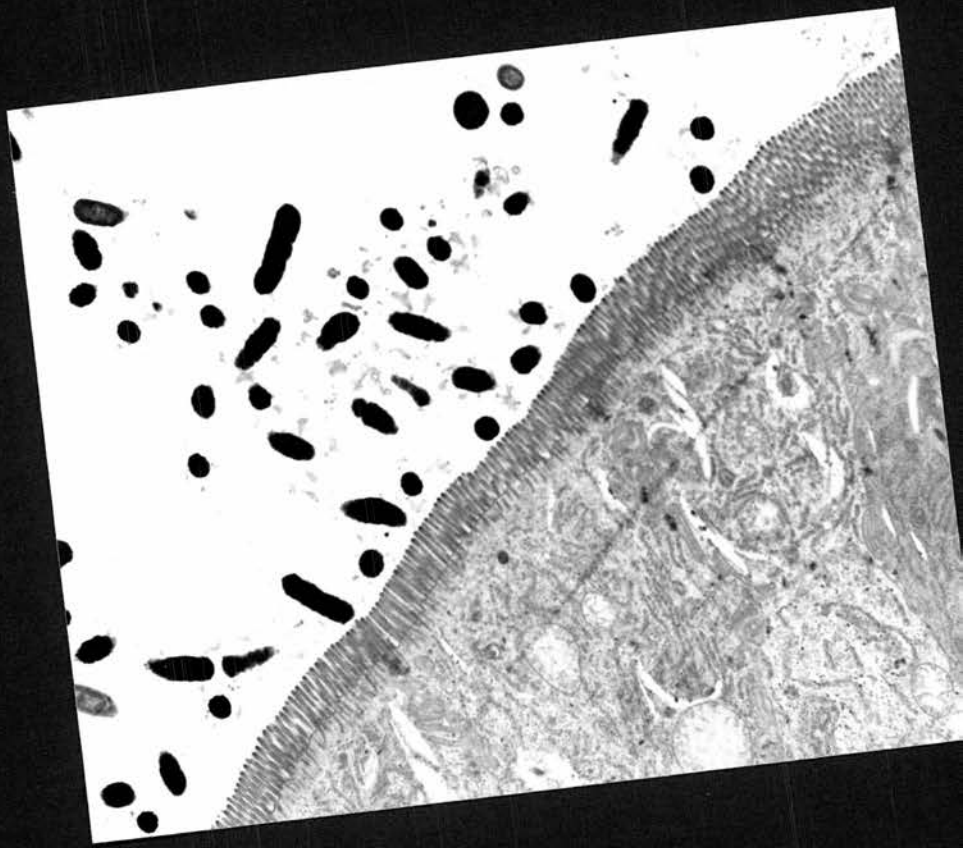

Figure 7.19. Piglet 195/80, site 4. Transmission electron micrograph showing mixed bacterial flora in close association with surface of host enterocytes. Note attached cryptosporidia. Final magnification = 3,870.

Figure 7.20. BA 195/80, site 4. High power transmission electron micrograph showing close association of bacteria, and a cryptosporidium, with the microvilli of a host enterocyte.
Final magnification = 41,000.